Journal of Paleontology, page 1 of 23

Published by Cambridge University Press
on behalf of Paleontological Society
0022-3360/24/1937-2337
doi: 10.1017/jpa.2024.16

JOURNAL OF PALEONTOLOGY
A PUBLICATION OF THE Paleontological SOCIETY

New materials of acanthomorphic acritarchs from the Ediacaran Weng'an Biota (South China)

Junxian Wu,[1,2] Weichen Sun,[1] Xiaodong Shang,[3] Pengju Liu,[3] Maoyan Zhu,[1,2,4] and Zongjun Yin[1,4]*

[1]State Key Laboratory of Palaeobiology and Stratigraphy, Nanjing Institute of Geology and Palaeontology, Chinese Academy of Sciences, Nanjing 210008, China <jxwu@nigpas.ac.cn> <wcsun@nigpas.ac.cn> <myzhu@nigpas.ac.cn> <zjyin@nigpas.ac.cn>
[2]College of Earth and Planetary Sciences, University of Chinese Academy of Sciences, Beijing 100049, China
[3]MNR Key Laboratory of Stratigraphy and Palaeontology, Institute of Geology, Chinese Academy of Geological Sciences, Beijing 100037, China <shangxiaodong13@mails.ucas.ac.cn> <pengju@cags.ac.cn>
[4]Nanjing College, University of Chinese Academy of Sciences, Nanjing 211135, China

Non-technical Summary.—The Weng'an Biota, found in the Doushantuo Formation in Guizhou Province, South China, is a remarkable fossil assemblage known for its well-preserved ancient life forms. These include small organisms called acritarchs, algae, and even embryo-like fossils. Among these, acritarchs, shaped like spiny spheres, have been essential for understanding the age and relationships of rocks from the Ediacaran Period. Previous studies mainly focused on larger spiny acritarchs, overlooking the smaller ones. In our study, we carefully examined over 500 thin sections and discovered a wealth of well-preserved small and medium-sized acritarchs. These tiny fossils, with diameters ranging 20–150 μm, help us understand the ancient ecosystems and how life evolved during this critical time in Earth's history. We identified several different species of small spiny acritarchs, e.g., *Tanarium conoideum*, *Tanarium elegans*, *Mengeosphaera membranifera*, *Mengeosphaera minima*, and *Variomargosphaeridium gracile*. Additionally, we found medium-sized acritarchs, e.g., *Tanarium tuberosum* and *Weissiella* cf. *W. grandistella*. These new findings provide important clues for correlating the rocks of the Doushantuo Formation in the Weng'an area with those in the Yangtze Gorges region. They also help us understand the evolution of acritarchs in different parts of the world, including Australia, Siberia, and the East European Platform.

Abstract.—The Weng'an Biota from the Ediacaran Doushantuo Formation in Guizhou Province, southwestern China, is known for its three-dimensionally phosphatized acritarchs, multicellular algae, and embryo-like animal fossils. Among these diverse microfossils, acanthomorphic acritarchs have played a significant role in the biostratigraphic subdivision and correlation of the lower-middle Ediacaran System. However, most previous studies on the biostratigraphy of the Doushantuo Formation in the Weng'an area have focused on large acanthomorphic acritarchs (LAAs, vesicle diameter >200 μm), whereas the smaller acanthomorphic acritarchs (SAAs, vesicle diameter <100 μm) from the Weng'an Biota have been largely overlooked. In this study, we examined >500 thin sections and discovered a large number of well-preserved, small (<100 μm) and medium-sized acanthomorphic acritarchs (MAAs, vesicle diameter ranging 100–200 μm). In total, we have identified SAAs in four genera and six species (*Tanarium conoideum* Kolosova, 1991, emend. Moczydłowska et al., 1993; *Tanarium elegans* Liu et al., 2014; *Mengeosphaera membranifera* Shang, Liu, and Moczydłowska, 2019; *Mengeosphaera minima* Liu et al., 2014; *Estrella recta* Liu and Moczydłowska, 2019; *Variomargosphaeridium gracile* Xiao et al., 2014), as well as two types of MAAs (*Tanarium tuberosum* Moczydłowska, Vidal, and Rudavskaya, 1993, emend. Moczydłowska, 2015; *Weissiella* cf. *W. grandistella* Vorob'eva, Sergeev, and Knoll, 2009, emend. Liu and Moczydłowska, 2019). This updated acritarch assemblage of the Weng'an Biota is valuable for correlating the Ediacaran Doushantuo Formation between the Weng'an and Yangtze Gorges areas. It also serves as a tool to test the proposed acritarch biozones in Ediacaran formations of South China and other localities, including Australia, Siberia, and the East European Platform.

Introduction

The Ediacaran Period witnessed the evolution of the Earth-Life system from Snowball Earth to the Cambrian explosion, making it one of the most critical transitional periods in the entire geological history (Narbonne et al., 2012; Xiao and Narbonne, 2020). Many important events in the evolution of life and the environment, e.g., the origin and early radiation of metazoans and the Neoproterozoic Oxygenation Event (NOE), occurred during the Ediacaran Period and left numerous significant geological records worldwide (e.g., Xiao and Knoll, 2000, 2007). Consequently, a broadly accepted internal subdivision scheme and chronostratigraphic framework for the Ediacaran System is

*Corresponding author.

essential, because it forms the basis for studying the coevolution of biology and the environment during this period. However to date, the internal subdivision scheme and a standard for regional stratigraphic correlation for the Ediacaran System are still under debate (Steiner et al., 2007; Liu et al., 2014b; Zhou et al., 2019; Zhu et al., 2019).

Ediacaran large acanthomorphic acritarchs (LAAs, with diameter normally > 200 μm) are globally distributed microfossils and exhibit high diversity, playing a crucial role in biostratigraphic subdivisions and correlation of the Ediacaran System (Vidal, 1990; Vorob'eva et al., 2009; Golubkova et al., 2010; Sergeev et al., 2011; Anderson et al., 2017). In 2005, Grey established five acritarch assemblage zones based on LAA fossils for the Ediacaran System of Australia (Grey, 2005), and this scheme has gained support from other studies (Willman et al., 2006; Willman and Moczydłowska, 2008, 2011; Sergeev et al., 2011), indicating that LAAs could be a valuable tool for the internal subdivision and global correlation of the Ediacaran System.

Since the 1970s, abundant LAAs have been discovered in the Ediacaran Doushantuo Formation in South China (Yin and Li, 1978; McFadden et al., 2009; Liu et al., 2014a; Liu and Moczydłowska, 2019). Based on extensive investigation of taxonomic diversity, Liu and Moczydłowska (2019) established four acritarch assemblage zones for the Ediacaran Doushantuo Formation in the Yangtze Gorges area. However, biostratigraphic correlation between the Ediacaran Doushantuo Formation of Yangtze Gorges area, South China, and the Ediacaran Pertatataka and Julie formations of Australia has long been difficult due to two reasons. First, silicified acanthomorphic acritarchs from chert nodules (Xiao et al., 2010) revealed by thin sections look different from carbonaceous acritarchs extracted from shales using acid maceration, even for the same species. Second, many acritarchs are mainly local species with limited significance in global biostratigraphic correlations. Therefore, how to correlate Ediacaran acritarch assemblage zones of South China with that of Australia, Siberia, and the Eastern European Platform remains uncertain. To resolve the problem, more investigations on acritarch diversity and taxonomy are needed. In addition, although previous studies have established four acritarch assemblage zones for the Ediacaran Doushantuo Formation in the Yangtze Gorges area (Liu and Moczydłowska, 2019), it remains uncertain whether the scheme of these four biozones is applicable to the Ediacaran Doushantuo Formation in the Weng'an area.

In this study, we focused on the fossil assemblage of acanthomorphic acritarchs from the Ediacaran Doushantuo Formation in the Weng'an area of Guizhou Province, southwestern China. Unlike many small acanthomorphic acritarchs (SAAs, with diameters < 100 μm) found in other regions, e.g., the Yangtze Gorges area in South China, Australia, Siberia, and the East European Platform, the majority of acanthomorphic acritarchs reported previously from the Weng'an Biota have diameters > 200 μm. For instance, *Tianzhushania* Yin and Li, 1978, emend. Yin, Zhou, and Yuan, 2008 and *Yinitianzhushania* Xiao et al., 2014a have diameters that can exceed 600 μm. To date, a total of 25 genera and 47 species plus two undetermined species of acanthomorphic acritarchs (Table 1) have been described from the Weng'an Biota. Among them, 22 genera and 28 species belong to the LAAs. It is noteworthy that only eight genera and 10 species plus one undetermined genus of SAAs have been discovered in the Weng'an Biota (L. Yin et al., 2011). Additionally, seven genera and eight species of medium-sized acritarchs (MAAs, with diameters ranging 100–200 μm) have been identified (Xiao et al., 2014a). The Weng'an SAAs include *Appendisphaera grandis* Moczydłowska, Vidal, and Rudavskaya, 1993, emend. Moczydłowska, 2005; *Bullatosphaera* sp. indet.; *Dicrospinasphaera virgata* Grey, 2005; *Dicrospinasphaera zhangii* Yuan and Hofmann, 1998; *Eotylotopalla delicata* Yin, 1987; *Hocosphaeridium anozos* (Willman in Willman and Moczydłowska, 2008) Xiao et al., 2014a; *Mengeosphaera chadianensis* (Chen and Liu, 1986) Xiao et al., 2014a; *Tanarium digitiforme* (Nagovitsin and Faizullin in Nagovitsin et al., 2004) Sergeev, Knoll, and Vorob'eva, 2011; *Tanarium victor* Xiao et al., 2014a; *Taedigerasphaera lappacea* Grey, 2005; and *Variomargosphaeridium gracile* Xiao et al., 2014a. The MAAs include *Asterocapsoides sinensis* Yin and Li, 1978, emend. Xiao et al., 2014a; *Asterocapsoides wenganensis* (Chen and Liu, 1986) Xiao et al., 2014a; *Cavaspina acuminata* (Kolosova, 1991) Moczydłowska, Vidal, and Rudavskaya, 1993; *Eotylotopalla dactylos* Zhang et al., 1998; *Ericiasphaera rigida* Zhang et al., 1998; *Mengeosphaera reticulata* (Xiao and Knoll, 1999) Xiao et al., 2014a; *Papillomembrana boletiformis* Xiao et al., 2014a; and *Taeniosphaera doushantuoensis* Liu and Yin, 2005 (Table 1). Considering that the diversity of small and medium-sized acritarchs in the Weng'an Biota has not been fully explored, this study focuses on them to uncover additional clues for Ediacaran biostratigraphic correlation.

Geological setting

Geological investigation of the Doushantuo Formation in the Weng'an area started in the 1960s (Xiao et al., 2014b). The Doushantuo Formation in the Weng'an phosphorite mining area, located in Guizhou Province, southwestern China (Fig. 1.1), outcrops in a pattern controlled by a north/northeast to south/southwest-trending Baiyan-Gaoping anticline (Fig. 1.2). A generalized stratigraphic column of the Doushantuo Formation in this area is displayed in Figure 1.3 (Xiao et al., 2014b; Cunningham et al., 2017). The entire formation is composed of five units, arranged from bottom to top as follows: cap dolomite (Unit 1), the lower phosphorite (Unit 2), the middle dolomite (Unit 3), the upper phosphorite (Unit 4), and the phosphoritic dolomite members (Unit 5). Detailed description of lithostratigraphy for the Doushantuo Formation in the Weng'an area can be found in numerous previous publications (Xiao et al., 1998, 2014a; Yin et al., 2015; Zhou et al., 2017).

The Weng'an Biota was described from the upper phosphorite (Unit 4), which consists of the lower black phosphorite facies (Unit 4A) and upper gray phosphatic dolomite facies (Unit 4B). Although the depositional age range for the Doushantuo Formation is well dated, ranging 635–551 Ma (Condon et al., 2005), the Weng'an Biota has long lacked precise isotopic age constraints. There are two karstic surfaces that have developed in the Doushantuo Formation in the Weng'an area, one at the top of Unit 3 and the other within Unit 5 (Zhu et al., 2007, 2013, 2019). If the lower karstic surface can be correlated to the 582 Ma Gaskiers glaciation (Condon et al., 2005), then the Weng'an Biota would be younger than 582 Ma. However, if the

https://doi.org/10.1017/jpa.2024.16 Published online by Cambridge University Press

Table 1. Small and medium-sized acanthomorphs from the Doushantuo Formation in the Weng'an area, records from the published literature and this study. EEP = East European Platform; 1 = Chen, 2004; 2 = Chen and Liu, 1986; 3 = Chen et al., 2010; 4 = Golubkova et al., 2010; 5 = Grey, 2005; 6 = Knoll, 1992; 7 = Kolosova, 1991; 8 = Liu et al., 2012; 9 = Liu et al., 2014a; 10 = Liu and Moczydłowska, 2019; 11 = Moczydłowska, 2005; 12 = Moczydłowska and Nagovitsin, 2012; 13 = Moczydłowska et al., 1993; 14 = Nagovitsin et al., 2004; 15 = Sergeev et al., 2011; 16 = Veis et al., 2006; 17 = Vorob'eva et al., 2009; 18 = Vorob'eva et al., 2008; 19 = Willman and Moczydłowska, 2008; 20 = Willman and Moczydłowska, 2011; 21 = Xiao, 2004; 22 = Xiao et al., 2014a; 23 = Xiao and Knoll, 1999; 24 = Xiao et al., 1999; 25 = Xie et al., 2008; 26 = Yin, 1987; 27 = Yin, 1990; 28 = Yin and Li, 1978; 29 = C. Yin et al., 2011; 30 = Yin et al., 2007; 31 = L. Yin et al., 2011; 32 = Yin et al., 2013; 33 = Yuan and Hofmann, 1998; 34 = Yuan et al., 2002; 35 = Zang and Walter, 1992; 36 = Zhang et al., 1998; 37 = Zhou et al., 2001; 38 = Zhou et al., 2002a; 39 = Zhou et al., 2007; 40 = Zhou et al., 2002b; 41 = Zhou et al., 2004; 42 = Shang et al., 2019; 43 = Ouyang et al., 2021; * = diameter < 100 μm; ** = medium-sized acritarchs reported by this study; # = species reported previously with diameter <100μm.

Taxa	Doushantuo (Weng'an)	Douschantuo (elsewhere in South China	Australia	Siberia	Other
Appendisphaera grandis Moczydłowska, Vidal, and Rudavskaya, 1993#	(22)	Zhangcunping (3)	(19)	(4, 13, 13)	-
Asterocapsoides sinensis Yin L. and Li, 1978	(22, 34)	Yangtse Gorges area (28, 36) Chaoyang (37)	–	–	EEP (17)? Svalbard (6)
Asterocapsoides wenganensis (Chen and Liu, 1986)	(2, 22, 33) This study	Baokang (40–42)	–	–	–
Bullatosphaera sp. indet.#	(22)	–	–	–	–
Cavaspina acuminata (Kolosova, 1991)	(22, 30, 32, 34) This study	Xiaofenge (36) Changyang (30) Baokang (10, 42)	(19, 20)	(11–14)	EEP (16, 17)
Dicrospinasphaera virgata Grey, 2005#	(22, 31)	–	–	–	–
Dicrospinasphaera zhangii Yuan and Hofmann, 1998#	(22, 30, 31, 33, 34)	Yangtze Gorges (21)	–	–	–
Eotylotopalla dactylos Zhang et al., 1998	(22)	Xiaofenghe (29, 34, 36) Tianjiayuanzi (39)	–	–	–
Eotylotopalla delicata Yin, 1987#	(31)	Yangtze Gorges (8, 26, 27, 29, 30, 34, 36)	–	–	–
Ericiasphaera rigida Zhang et al., 1998	(22, 30, 34, 36)	Yangtze Gorges (17)	–	–	–
Estrella recta Liu and Moczydłowska, 2019*	This study	Xiaofenghe (10)	–	–	–
Hocosphaeridium anozos (Willman in Willman and Moczydłowska, 2008)#	(22)	–	(5, 19, 35)	–	–
Mengeosphaera chadianensis (Chen and Liu, 1986)#	(1, 18, 22)	Yangtze Gorges (25, 30) Mianxian (1, 23, 24, 36, 40) Baokang (37, 41) Chaoyang (38)	–	–	–
Mengeosphaera membranifera Shang, Liu, and Moczydłowska, 2019 *	This study	Liujing section (42)	–	–	–
Mengeosphaera minima Liu et al., 2014a*	This study	Niupin (9)	–	–	–
Mengeosphaera reticulata (Xiao and Knoll, 1999)	(1, 22, 23, 30)	–	–	–	–
Papillomembrana boletiformis Xiao et al., 2014a	(22)	–	–	–	–
Taedigerasphaera lappacea Grey, 2005	(31)	–	(5)	–	–
Taeniosphaera doushantuoensis Liu and Yin, 2005	(5, 19)	–	–	–	–
Tanarium conoideum Kolosova, 1991*	(22) This study	Yangtze Gorges area (9)	–	(7, 11–13, 15)	–
Tanarium digitiforme (Nagovitsin and Faizullin in Nagovitsin et al., 2004) #	(22) This study	Yangtze Gorges area (43)	(5, 15)	(4, 12, 14, 15, 18)	–
Tanarium elegans Liu et al., 2014a*	This study	Xiaofenghe (9)	–	–	–
Tanarium tuberosum Moczydłowska, Vidal, and Rudavskaya, 1993**	This study	Yangtze Gorges area (9, 42)	(19)	(7, 11, 13, 16)	EEP (17)
Tanarium victor Xiao et al., 2014a #	(22)	–	–	–	–
Variomargosphaeridium gracile Xiao et al., 2014a*	(22, 30) This study	Yangtze Gorges (9)	–	–	–
Weissiella cf. *W. grandistella* Vorob'eva, Sergeev, and Knoll, 2009**	This study	–	–	–	EEP (17)

upper karstic surface correlates to the Gaskiers glaciation (Xiao et al., 2014a), then the Weng'an Biota would be much older than 582 Ma. A U-Pb age of 609 ± 5 Ma, determined from the ash bed immediately above Unit 4 of the Ediacaran Doushantuo Formation at the Zhancunping section in Hubei Province, correlates with Unit 4A of the Ediacaran Doushantuo Formation at the Weng'an area. This age constraint provides important chronological information for the Weng'an Biota (Zhou et al., 2019). However, based on new CA-ID-TIMS U-Pb analyses, Yang et al. (2021) claimed that zircons from the same ash bed have a detrital origin with maximum depositional age of 612.5 ± 0.9 Ma. Through chemo- and biostratigraphic correlation, Yang et al. (2021) proposed that the age of the Weng'an Biota likely ranges 575–590 Ma.

https://doi.org/10.1017/jpa.2024.16 Published online by Cambridge University Press

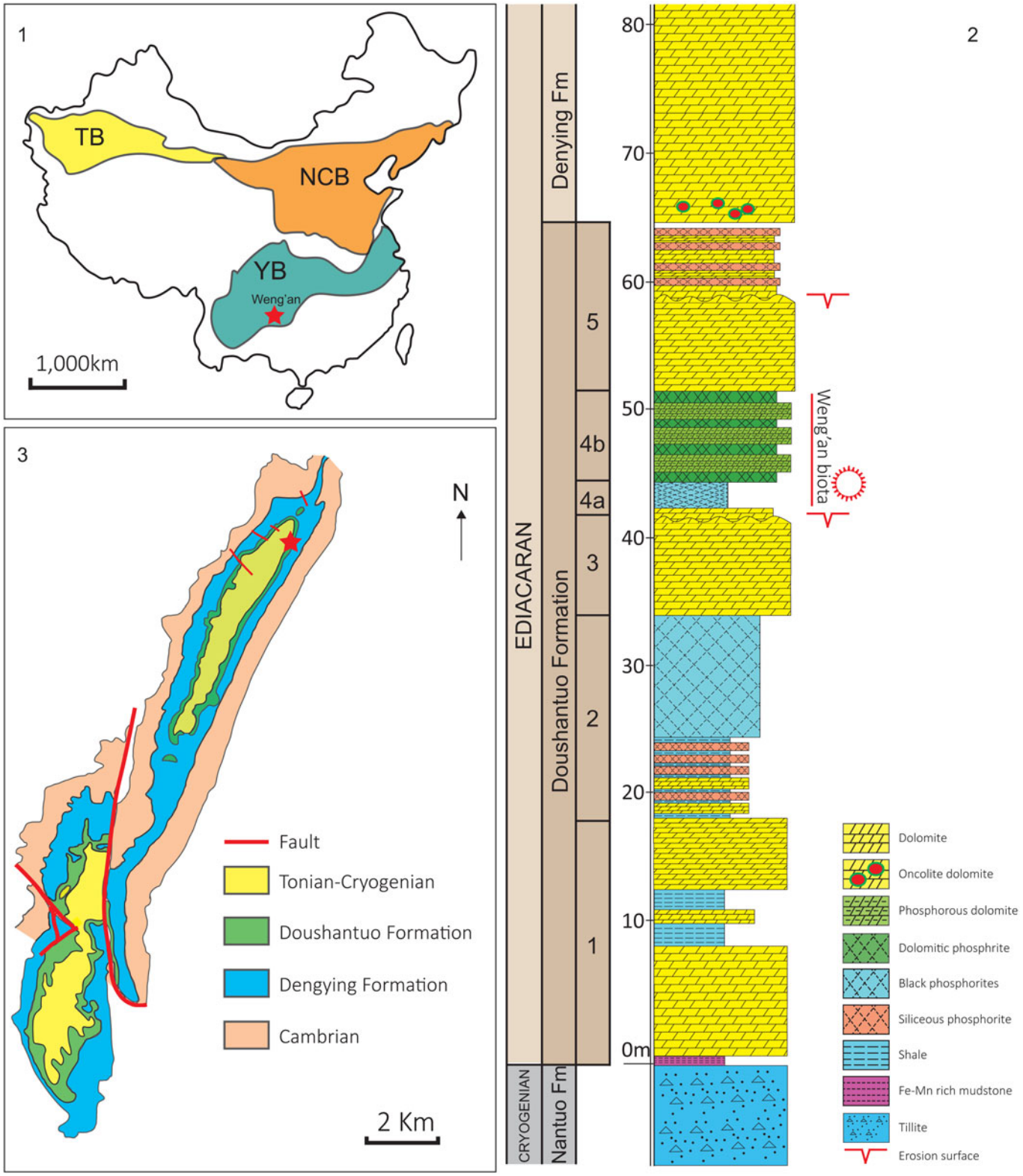

Figure 1. The geological setting of Weng'an area. (**1**) Relationships between the Yangtze Block (YB), North China Block (NCB), and Tarim Block (TB). A red star marks the locality of the Weng'an phoshorite mining area. (**2**) Geological setting of the Weng'an area; the outcrop is marked by a red star. (**3**) Ediacaran stratigraphic column of the Beidoushan section in the Weng'an area showing the fossil horizon. Modified from Yin et al., 2015.

https://doi.org/10.1017/jpa.2024.16 Published online by Cambridge University Press

Materials and methods

The specimens reported in this study were collected from the black phosphorite facies (Unit 4A) of the Doushantuo Formation in the Weng'an area (Fig. 1.3). More than 500 thin sections were examined to search for microfossils under a transmitted light microscope (Nikon Ni-U microscope). All acanthomorphic acritarchs revealed in thin sections were recorded with stage coordinates, and then photographed with a Nikon FIT-1 CCD camera. Measurements for vesicle diameter, length, quantity, and basal width of processes were conducted on high-resolution photographs using Image J (http://imagej.nih.gov/ij); the measured data are provided in Appendix 1.

Repository and institutional abbreviation.—Microfossils illustrated here are reposited at the Nanjing Institute of Geology and Palaeontology, Chinese Academy of Science, Nanjing, China (NIGPAS).

Systematic paleontology

In this study, we adhered to the criteria established by Xiao et al. (2014a) to define vesicle size, which is quantitatively diagnosed as small (<100 μm diameter), medium-sized (100–200 μm diameter), or large (>200 μm diameter). In acritarch taxonomy, the characteristics of processes (e.g., morphology, density, branching, and whether hollow processes communicate with the vesicle interior; Fig. 2) play a significant role. A systematic description is given in alphabetic order for acanthomorphic acritarch taxa below.

Group Acritarcha Evitt, 1963
Genus *Estrella* Liu and Moczydłowska, 2019

Type species.—*Estrella greyae* Liu and Moczydłowska, 2019 from the Yangtze Gorges area, northern Xiaofenghe section, South China.

Estrella recta Liu and Moczydłowska, 2019
Figures 2.1, 3

2019 *Estrella recta* Liu and Moczydłowska, p. 109, fig. 57A–F.

Holotype.—Thin section nos. IGCAGS-D2XFH200 and XFH0946-1-9, F48/4 from the Yangtze Gorges area, Nantuocun section, Member II of the Doushantuo Formation, South China (Liu and Moczydłowska, 2019, p.108, fig. 57A–D).

Description.—Small-sized spherical vesicle with an irregular outline resulting from collapse during taphonomic and diagenetic processes, bearing homomorphic and regularly distributed hollow processes. The processes are elongated tubular structures that taper toward their distal portions, ending in sharp tips. They are hollow and freely communicate with the vesicle cavity. The widened bases of processes create a wavy outline of the vesicle wall. Vesicle diameter 35–48 μm (mean 43 μm, N = 3); process length 8–27 μm (mean 19 μm, N = 47); process basal width 2–11 μm (mean 5 μm, N = 14); distance between processes 6–12 μm (mean 9 μm, N = 13); ~16–25 processes on the vesicle periphery in circumferential view.

Material.—Five well-preserved specimens and one poorly preserved specimen from Unit 4A of the Ediacaran Doushantuo Formation in the Weng'an area.

Remarks.—The species is distinguished by its robust hollow processes, characterized by an elongate conical shape and bulbous bases. Vesicles exhibit a circular shape with a slightly undulating outline (Fig. 3). Due to taphonomy and diagenesis, many specimens have undergone deformation. Consequently in some specimens, the length of processes exceeds the vesicle diameter, whereas in others, the length of processes is only half of the vesicle diameter. Although sharing similarities in vesicle size and process length with several species of the genus *Tanarium* Kolosova, 1991—e.g., *Tanarium gracilentum* (Yin in Yin and Liu, 1988) Ouyang et al., 2021, *Tanarium pycnacanthum* Grey, 2005, and *Tanarium paucispinosum* Grey, 2005—the species differs in process morphology and density. Both *Tanarium gracilentum* and *Tanarium pycnacanthum* feature more densely distributed processes (>100 processes in circumferential view). In contrast, *Tanarium paucispinosum* (with <10 processes in circumferential view) possesses more slender and more flexible processes compared to our specimens. Consequently, our specimens are classified as *Estrella recta*.

Genus *Mengeosphaera* Xiao et al., 2014a

Type species.—*Mengeosphaera chadianensis* (Chen and Liu, 1986) Xiao et al., 2014a from the Doushantuo Formation at Weng'an area, South China.

Mengeosphaera membranifera Shang, Liu, and Moczydłowska, 2019
Figures 2.2, 4

2019 *Mengeosphaera membranifera* Shang et al., p. 18, fig. 15A–D.

Holotype.—Thin section no. LJ101115-1-7 from the Songlin area of Guizhou Province, Liujing section of chert nodules in medium- to thick-bedded dolostones of the Ediacaran Doushantuo Formation, South China (Shang et al., 2019, p. 18, fig. 15A–D).

Description.—Small spheroidal vesicles exhibiting abundant, closely, and regularly arranged biform processes of uniform length, each surrounded by an outer membrane. The outer membrane is supported by processes, and the distance from the outer membrane to the bases of the processes remains constant within a single specimen. Processes consist of regular conical bases and cylindrical, thin apical spines with sharp tips. They are hollow and freely communicate with the vesicle interior. Vesicle diameter 40–48 μm (mean 43 μm, N = 4); process length 4–7 μm (mean 6 μm, N = 185); process basal width 1–2 μm (mean 2 μm, N = 17); distance between

https://doi.org/10.1017/jpa.2024.16 Published online by Cambridge University Press

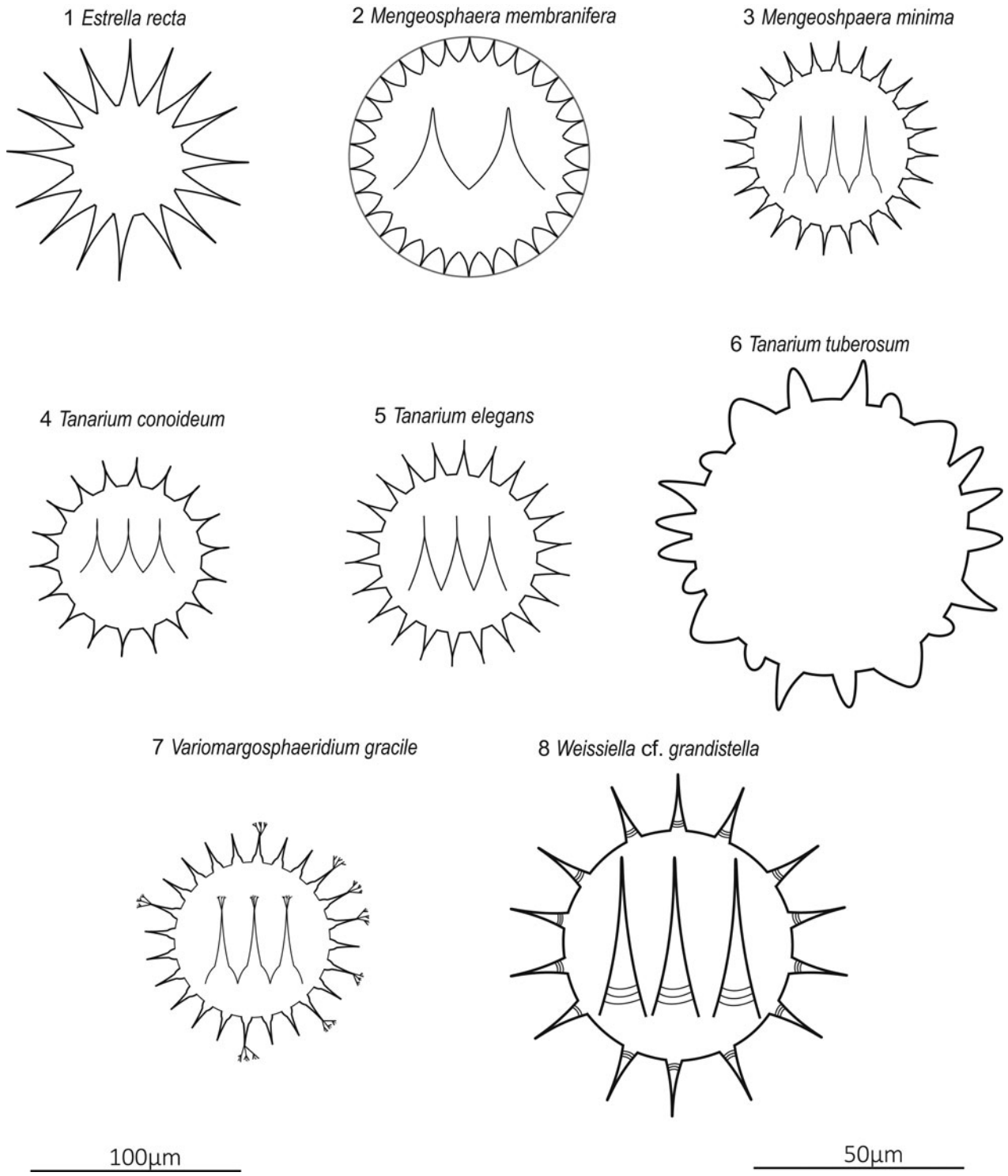

Figure 2. Schematic drawings of acritarchs: (**1**) *Estrella recta* Liu and Moczydłowska, 2019; (**2**) *Mengeosphaera membranifera* Shang, Liu, and Moczydłowska, 2019; (**3**) *M. minima* Liu et al., 2014a; (**4**) *Tanarium conoideum* Kolosova, 1991; (**5**) *Tanarium elegans* Liu et al., 2014a; (**6**) *Tanarium tuberosum* Moczydłowska, Vidal, and Rudavskaya, 1993, emend. Moczydłowska, 2015; (**7**) *Variomargosphaeridium gracile* Xiao et al., 2014a; (**8**) *Weissiella* cf. *W. grandistella* Vorob'eva, Sergeev, and Knoll, 2009, emend. Liu and Moczydłowska, 2019. The left scale bar is for (**6**) and (**8**); the right scale bar is for the others.

processes 1–4 µm (mean 3 µm, N = 19); ~40 processes in circumferential view.

Material.—Five specimens from Unit 4A of the Ediacaran Doushantuo Formation in the Weng'an area.

Remarks.—Acritarchs featuring an outer membrane supported by biform processes are rare in the Ediacaran Period, with known occurrences limited to chert nodules in the Liujing section, Songlin area of Guizhou Province, southwestern China (Shang et al., 2019). Our specimens exhibit similarities

https://doi.org/10.1017/jpa.2024.16 Published online by Cambridge University Press

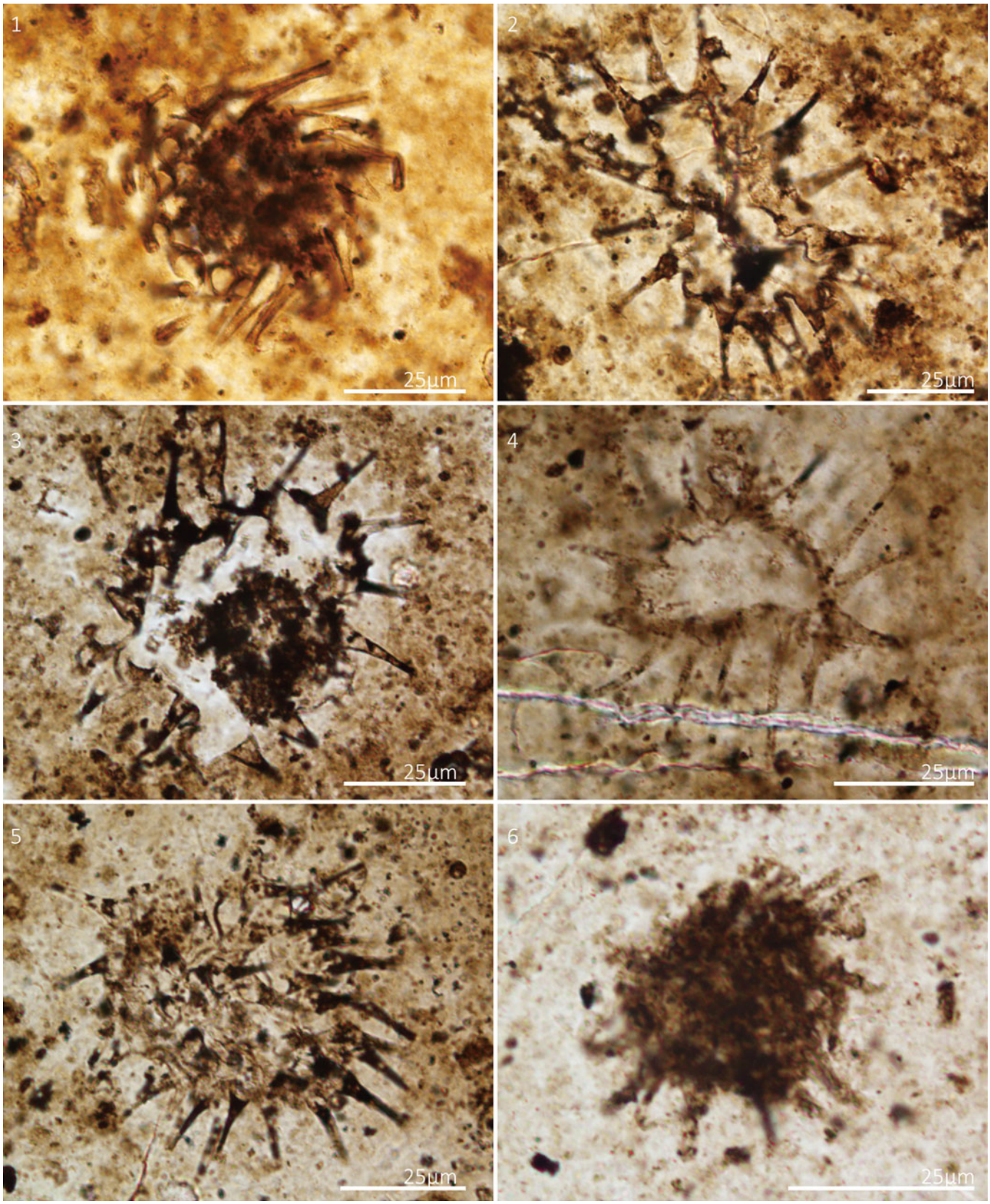

Figure 3. *Estrella recta* Liu and Moczydłowska, 2019. Thin section numbers: (**1**) WS17-225-X42Y105, (**2**) WS17-225-X46Y106, (**3**) WS17-195-X54Y99, (**4**) WS17-157-X64Y101, (**5**) WS17-259-X19.5Y113, (**6**) WS17-211-X35Y94.

https://doi.org/10.1017/jpa.2024.16 Published online by Cambridge University Press

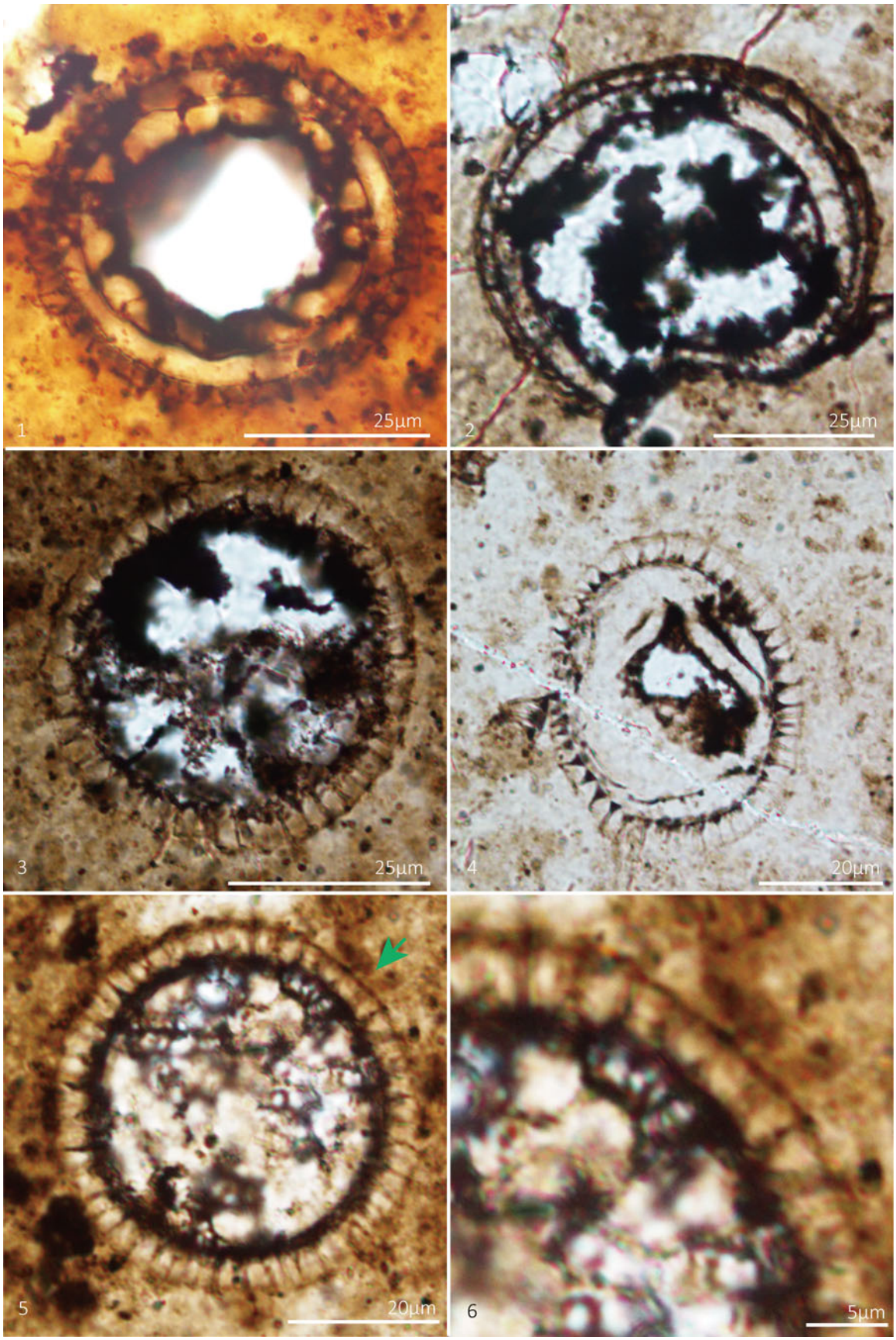

Figure 4. *Mengeosphaera membranifera* Shang, Liu, and Moczydłowska, 2019. Thin section numbers: (**1**) WS17-152-X62Y103, (**2**) WS17-231-X64Y108, (**3**) WS17-231-X27Y101, (**4**) WS17-204-X37Y93, (**5**) WS17-207-X30Y104, with green arrow indicating site of (**6**), (**6**) magnified view of (**5**).

https://doi.org/10.1017/jpa.2024.16 Published online by Cambridge University Press

to some *Mengeosphaera gracilis* Liu et al., 2014a in terms of process morphology and share resemblance with species of *Cymatiosphaeroides* (Knoll, 1984) Knoll, Swett, and Mark, 1991 in the outer membrane structure. However, they differ from *Mengeosphaera gracilis* due to the presence of the outer membrane and are distinguished from *Cymatiosphaeroides* by their distinct biform processes. Therefore, despite its smaller size compared to the specimens described by Shang et al. (2019), our specimens align more closely with the diagnostic features of *Mengeosphaera membranifera.*

Mengeosphaera minima Liu et al., 2014a
Figures 2.3, 5, 6

2014a *Mengeosphaera minima* Liu et al., p. 69, 101, figs. 51.8, 63.
2021 *Mengeosphaera minima*; Ouyang et al., p. 24, fig. 17M, N.
2022 *Mengeosphaera minima*; Ye et al., p. 52, fig. 32G, H.

Holotype.—Thin section no. I IGCAGS-NPIII-090A from the Yangtze Gorges area, Niuping section of the upper Member III, Doushantuo Formation, South China (Liu et al., 2014a, p. 69, fig. 63.1).

Description.—Small spheroidal vesicle bearing abundant, closely, and evenly distributed biform processes. Each process consists of a conical base and a thin apical filament. Occasionally, the apical spine is curved at the distal end (Figs. 5.1, 5.3, 6.1, 6.4, white arrows). The processes are hollow and freely communicate with the vesicle interior. Some specimens show multicellular structure (Fig. 6.1, 6.2, blue arrows). Vesicle diameter 33–46 µm (mean 39 µm, N = 40); process length 5–13 µm (mean 8 µm, N = 1,432); process basal width 2–4 µm (mean 3 µm, N = 246); process spacing 3–6 µm (mean 4 µm, N = 233); ~21–60 processes on vesicle periphery in circumferential view.

Material.—Forty-two specimens from Unit 4A of the Ediacaran Doushantuo Formation in the Weng'an area.

Remarks.—The specimens illustrated in Figures 5 and 6 align with the diagnostic criteria of *Mengeosphaera minima* (Liu et al., 2014a; Ouyang et al., 2021; Ye et al., 2022). The presence of the curved spine might be a taphonomic artifact, because this feature was not consistently observed. Although approximately a dozen species of *Mengeosphaera* exhibit conical expansion of the process bases (please refer the fig. 51 and table 2 in Liu et al., 2014a), only *M. bellula* Liu et al., 2014a, *M. minima*, *M. spicata* Xiao et al., 2014a, and *M. stegosauriformis* Xiao et al., 2014a share small vesicle sizes comparable to our specimens. Notably, the basal parts of the processes in *M. spicata* and *M. stegosauriformis* are larger (basal width 7–20 µm for *M. spicata* and 20–22 µm for *M. stegosauriformis*, according to Liu et al., 2014a). Additionally, *M. bellula* displays a different conical shape than *M. minima.*

Genus *Tanarium* Kolosova, 1991, emend. Moczydłowska et al., 1993

Type species.—*Tanarium conoideum* Kolosova, 1991, emend. Moczydłowska, et al., 1993, from the Ediacaran (Vendian) Kursov Formation in the Yakutia area of the Siberian Platform (Kolosova, 1991; Moczydłowska et al., 1993; Moczydłowska, 2005).

Tanarium conoideum Kolosova, 1991, emend. Moczydłowska et al., 1993
Figures 2.4, 7

1991 *Tanarium conoideum* Kolosova, p. 56, 57, fig. 5.1–5.3.
1993 *Tanarium conoideum*; Moczydłowska et al., p. 514–516, fig. 10C, D.
2014a *Tanarium conoideum*; Liu et al., p. 109, figs. 76.2, 77.1–77.6.
non 2016 *Tanarium conoideum*; Prasad and Ramson, 2016, p. 56, pl. 7, fig. 8.
2019 *Tanarium conoideum*; Shang et al., p. 26, fig. 16A–E.
non 2020 *Tanarium conoideum*; Yang et al., p. 6, 7, fig. 2K.
2020 *Tanarium conoideum*; Vorob'eva and Petrov, p. 374, 375, pl. 1, fig. 15.
2020 *Tanarium conoideum*; Yang et al., p. 8, fig. 2K.
2022 *Tanarium conoideum*; Ye et al., p. 61, fig. 42.

Holotype.—Thin section no. YIGS Nr 87-115 from the Kursov Formation, Upper Proterozoic, Vendian of Yakulia, Siberian Piatform and Borehole Byk-Tanar area (Kolosova, 1991, p. 56, fig. 5.1, 5.2).

Description.—Small spherical vesicles, bearing a small number of conical processes. The bases of the processes are slightly expanded and distally tapered to a pointed tip, or sometimes blunt due to breakage. The processes are hollow, allowing for free communication with the vesicle interior. Vesicle diameter 33–45 µm (mean 40 µm, N = 6); process length 8–10 µm (mean 7 µm, N = 89); process basal width 3–4 µm (mean 4 µm, N = 27); distance between processes 5–8 µm (mean 7 µm, N = 35); ~7–27 processes on the vesicle periphery in circumferential view.

Material.—Six specimens from Unit 4A of the Ediacaran Doushantuo Formation in the Weng'an area.

Remarks.—Most processes are straight, with a few showing distal hooks (Fig. 7.2, 7.3, white arrows). According to Xiao et al. (2014a), distally hooked processes can result from taphonomic alteration. Although the specimens in our collection are smaller than those previously reported for *Tanarium conoideum*, the process features align more closely with the diagnosis of *Tanarium conoideum* than with other species. The specimens diagnosed as *Tanarium conoideum* by Moczydłowska and Nagovitsin (2012) and Prasad and Ramson (2016), exhibit thin, short processes that are inconsistent with the diagnosis of *Tanarium conoideum*. Similarly, the specimen described as *Tanarium conoideum* by Yang et al. (2020) has abundant, relatively short, densely distributed processes with basal expansions, leading to its exclusion from *Tanarium conoideum.*

Tanarium elegans Liu et al., 2014a
Figures 2.5, 8.1, 8.2

2014a *Tanarium elegans* Liu et al., p. 81, fig. 75.8–75.16.

https://doi.org/10.1017/jpa.2024.16 Published online by Cambridge University Press

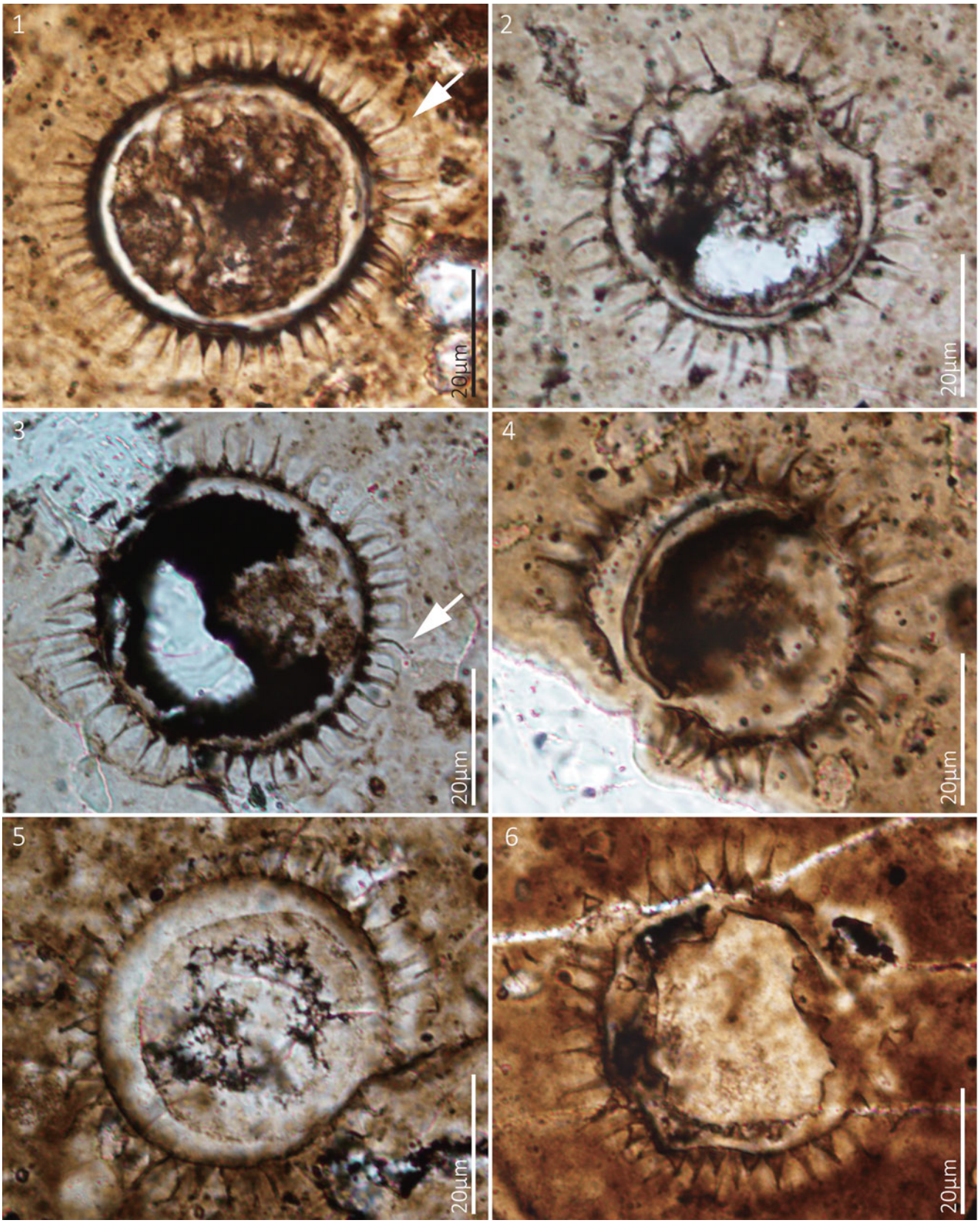

Figure 5. *Mengeosphaera minima* Liu et al., 2014a. Thin section numbers: (**1**) WS17-217-X48Y101, (**2**) WS17-153-X31Y91, (**3**) WS17-227-x57y97, (**4**) WS17-227-X46Y99, (**5**) WS17-231-X58Y112, (**6**) WS17-145-X50Y98.

https://doi.org/10.1017/jpa.2024.16 Published online by Cambridge University Press

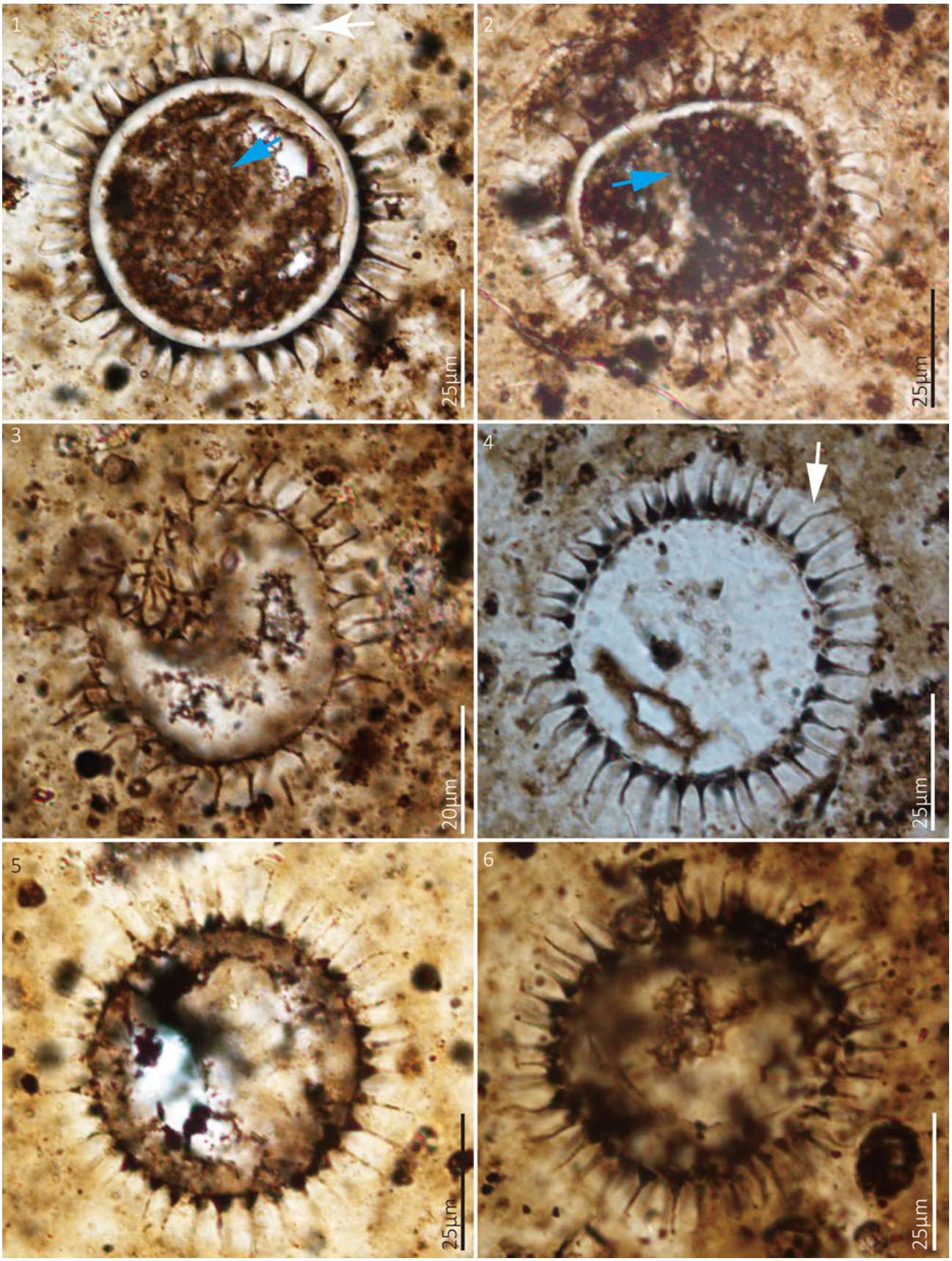

Figure 6. *Mengeosphaera minima* Liu et al., 2014a. Thin section numbers: (**1**) WS17-224-X45Y110, (**2**) WS17-235-X59Y107, (**3**) WS17-207-x17y99, (**4**) WS17-256-X36Y114, (**5**) WS17-220-X38Y100, (**6**) WS17-219-X25Y101. (**1, 2**) showing the multicellular structures within their vesicle (blue arrows).

https://doi.org/10.1017/jpa.2024.16 Published online by Cambridge University Press

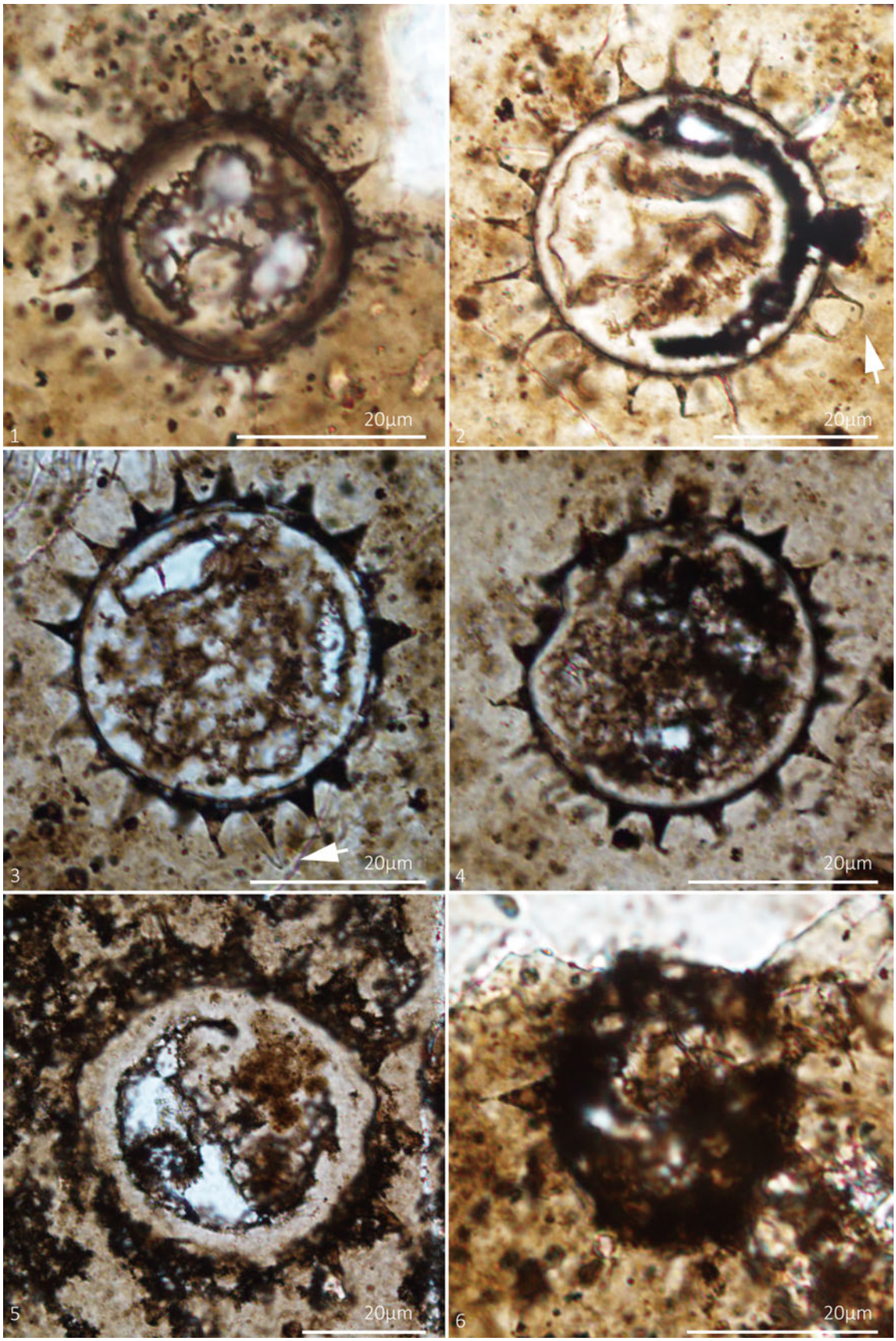

Figure 7. *Tanarium conoideum* Kolosova, 1991, emend. Moczydłowska et al., 1993. Thin section numbers: (**1**) WS17-210-X38Y103, (**2**) WS17-150-X47Y101, (**3**) WS17-234-X46Y99, (**4**) WS17-206-X25Y104, (**5**) WS17-208-X48Y98, (**6**) WS17-150-X50Y111.

https://doi.org/10.1017/jpa.2024.16 Published online by Cambridge University Press

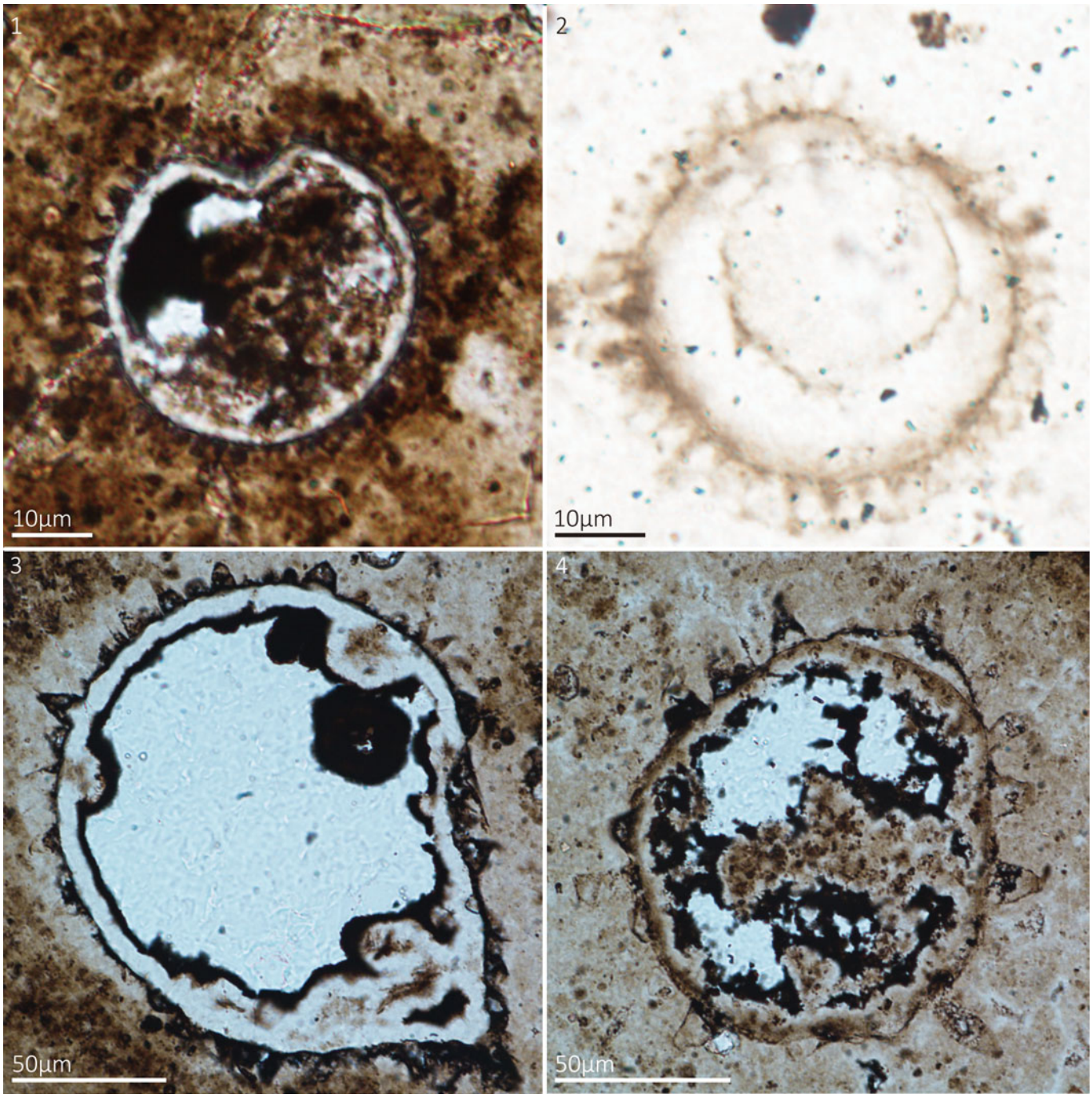

Figure 8. (**1, 2**) *Tanarium elegans* Liu et al., 2014a and (**3, 4**) *Tanarium tuberosum* Moczydłowska, Vidal, and Rudavskaya, 1993, emend. Moczydłowska, 2015. Thin section numbers: (**1**) WS17-196-X40Y107, (**2**) WS17-150-X59.5Y108, (**3**) WS17-201-x42.5y93.5, (**4**) WS17-202-X57Y93.

Holotype.—Thin section no. IGCAGS–XFH–270 from the Yangtze Gorges area, Xiaofenghe section of the lower Member II, Doushantuo Formation, South China (Liu et al., 2014a, fig. 75.10).

Description.—Small spheroidal vesicles exhibiting numerous evenly and regularly arranged conical processes. These processes, hollow in nature, freely communicate with the vesicle interior, and taper gradually to a blunt termination. Vesicle diameter 39 and 44 μm (only two specimens discovered during this study); process length 6–9 μm (mean 7 μm, N = 36); process basal width 1–3 μm (mean 2 μm, N = 4); > 30 processes in circumferential view.

Material.—Two specimens from Unit 4A of the Ediacaran Doushantuo Formation in the Weng'an area.

Remarks.—The specimens illustrated in Figures 8.1 and 8.2 align with the diagnostic criteria of *Tanarium elegans*. *Tanarium elegans* exhibits closest similarities to *Tanarium*

https://doi.org/10.1017/jpa.2024.16 Published online by Cambridge University Press

acus Liu et al., 2014a and *Xenosphaera liantuoensis* Yin, 1987, emend. Liu et al., 2014a in terms of small vesicle size and very thin processes. However, when compared to *Tanarium elegans*, *Tanarium acus* features relatively fewer but longer processes whereas *Xenosphaera liantuoensis* has a larger vesicle and longer processes. In addition, it is noteworthy that *Tanarium elegans* typically lacks a thin filamentous tip.

Tanarium tuberosum Moczydłowska, Vidal, and Rudavskaya, 1993,
emend. Moczydłowska, 2015
Figures 2.6, 8.3, 8.4

1993 *Tanarium tuberosum* Moczydłowska et al., p. 516, fig. 15B–D.
2015 *Tanarium tuberosum*; Moczydłowska, pl. 3, figs. 1–6.
2016 *Tanarium tuberosum*; Prasad and Ramson, p. 56, 58, pl. 8, figs. 1, 2.
2019 *Tanarium tuberosum*; Liu and Moczydłowska, p. 153–156, fig. 86, pl. 21, fig. 18A.
2019 *Tanarium tuberosum*; Shang et al., p. 27–29, fig. 18.
2021 *Tanarium tuberosum*; Ouyang et al., p. 27, fig. 19R

Holotype.—Thin section no. PMU-Sib.4-J/30/3 from the Nepa-Botuoba area, lowermost Kbamaka Formation, Neoproterozoic, Upper Vendian (Moczydłowska et al., 1993, p. 516, fig. 15B–D).

Description.—Medium-sized spheroidal vesicle showcasing irregularly distributed wide conical processes. These processes, hollow and broad, feature blunt tips and freely communicate with the vesicle interior. Vesicle diameter 91 and 111 µm (only two specimens discovered during this study); process length 12–25 µm (mean 16 µm, N = 38); process basal width 6–11 µm (mean 9 µm, N = 14); distance between processes 6–23 µm (mean 14 µm, N = 11); ∼12–26 processes on vesicle periphery in circumferential view.

Material.—Two specimens from Unit 4A of the Ediacaran Doushantuo Formation in the Weng'an area.

Remarks.—The current specimens exhibit irregularly conical processes and a medium-sized vesicle diameter (91–111 µm). The vesicle size is comparable to the specimens featured by Liu and Moczydłowska (2019). There is a slight difference in the process number of the specimens in Figures 8.3 and 8.4 that could be interpreted as infraspecific variability (Liu and Moczydłowska, 2019).

Genus *Variomargosphaeridium* Zang and Walter, 1992, emend. Xiao et al., 2014a

Type species.—*Variomargosphaeridium litoschum* Zang and Walter, 1992, Doushantuo Formation at Weng'an area, South China; Amadeus Basin, Rodinga 4 borehole at a depth of 48.38–48.67 m, Pertatataka Formation, Ediacaran successions in Australia.

Variomargosphaeridium gracile Xiao et al., 2014a
Figures 2.7, 9

2014a *Variomargosphaeridium gracile* Xiao et al., p. 58, fig. 36.
2021 *Variomargosphaeridium gracile*; Ouyang et al., p. 31, fig. 22A.

Holotype.—Thin section no. Slide 87ZW15-4, CPC27760, from the Pertatataka Formation, Ediacaran successions in Australia (Zhang and Walter, 1992, p. 114, 117, figs. 63D–G, 88).

Description.—Small-sized spheroidal vesicle bearing evenly and densely distributed branching processes. These processes consist of conical bases and bifurcate tips, being thin, hollow, and freely communicating with the vesicle interior. Vesicle diameter 34–55 µm (mean 42 µm, N = 11); process length 6–13 µm (mean 10 µm, N = 449); process basal width 2–3 µm (mean 3µm, N = 84); distance between processes 3–5 µm (mean 4 µm, N = 87); ∼25–52 processes in circumferential view.

Material.—Thirteen specimens from Unit 4A of the Ediacaran Doushantuo Formation in the Weng'an area.

Remarks.—The specimens are identified as *Variomargosphaeridium gracile* based on vesicle size and process morphology. Although *V. litoschum* and *V. floridum* Nagovitsin and Moczydłowska in Moczydłowska and Nagovitsin, 2012 also exhibit branching processes, they are considerably larger in both vesicle and process sizes compared to our specimens (Grey, 2005; Moczydłowska and Nagovitsin, 2012; Xiao et al., 2014a). In addition, the processes of *V. floridum* branch distally to form an apical crown of branchlets, and the branching pattern of *V. litoschum* is more complex than that of *V. gracile* (Xiao et al., 2014a).

Genus *Weissiella* Vorob'eva, Sergeev, and Knoll, 2009, emend. Liu and Moczydłowska, 2019

Type species.—*Weissiella grandistella* Vorob'eva, Sergeev, and Knoll, 2009, emend. Liu and Moczydłowska, 2019 from the East European Platform and 2605.5 m depth of keltminsk 1 borehole, Ediacaran and Yangtze Gorges area, Doushantuo Formation.

Weissiella cf. *W. grandistella* Vorob'eva, Sergeev, and Knoll, 2009,
emend. Liu and Moczydłowska, 2019
Figures 2.8, 10

2009 *Weissiella grandistella* Vorob'eva, Sergeev, and Knoll, p. 183–185, figs. 10.1a–f.
2019 *Weissiella grandistella*; Liu and Moczydłowska, p. 163, figs. 91F, G, 92A–G.
2021 *Weissiella* cf. *W. grandistella*; Ouyang et al., p. 40, 41, fig. 24A–H.
2022 *Weissiella* cf. *W. grandistella*; Ye et al., p. 70, fig. 49D–F.

Holotype.—Thin section no. 14700-13, from the Ediacara, upper part of Vychegda Formation (Vorob'eva et al., 2009, p. 183–185, figs. 10.1a–f).

https://doi.org/10.1017/jpa.2024.16 Published online by Cambridge University Press

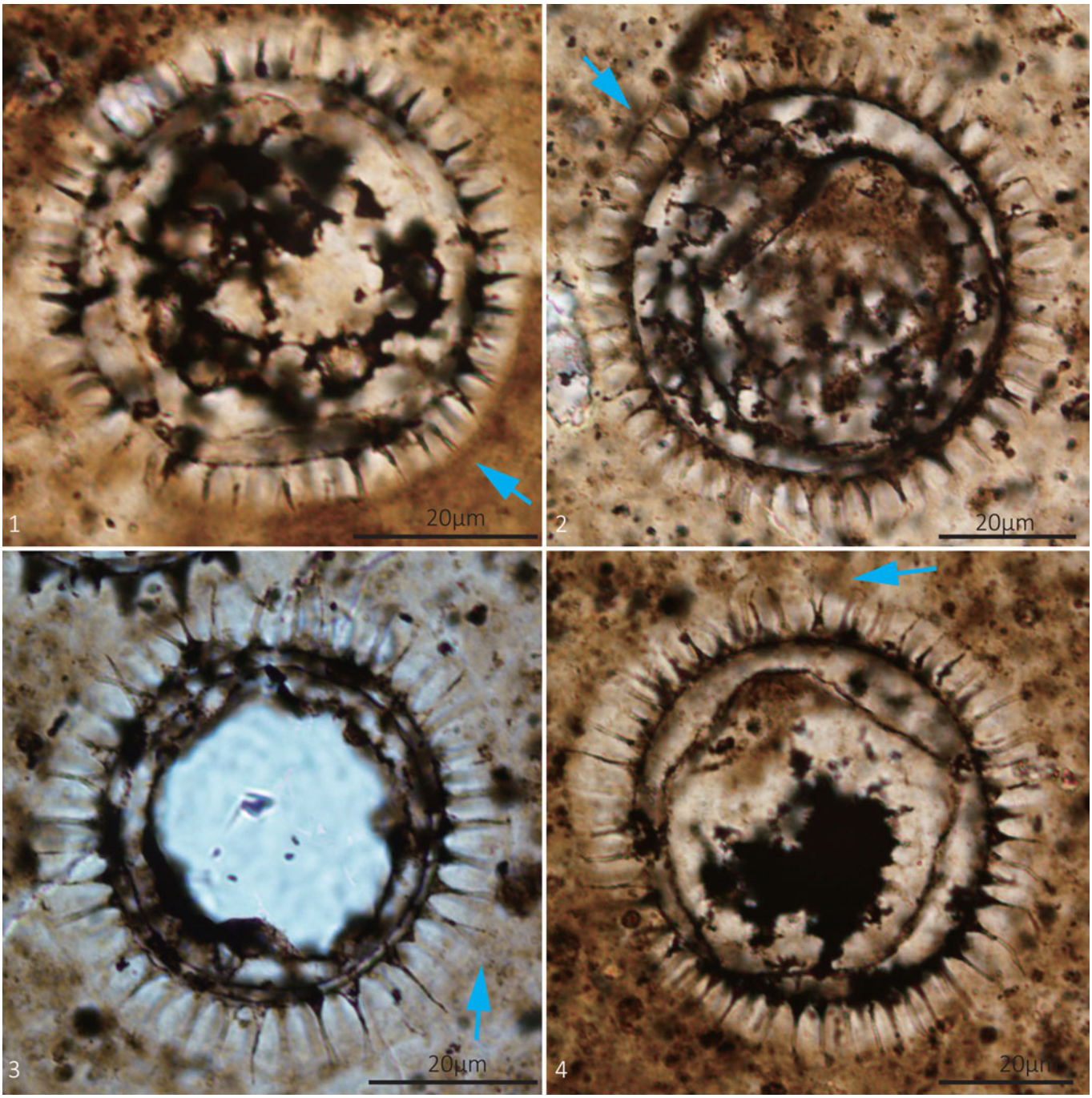

Figure 9. *Variomargosphaeridium gracile* Xiao et al., 2014a. Thin section numbers: (**1**) WS17-150-X50Y110, (**2**) WS17-161-X48Y103, (**3**) WS17-234-X46Y99, (**4**) WS17-207-X17Y99. These four specimens show bifurcated structures at the tops of the processes (blue arrows).

Description.—Medium-sized spheroidal vesicle featuring a few large processes. These processes, hollow and conical, exhibit a rounded or blunt end and have transverse crosswalls that are flat or distally convex. Vesicle diameter 118 μm (from specimen in Fig. 10.1); process length 33 μm (mean 33 μm, N = 4); process basal width 13 μm (mean 13 μm, N = 5); distance between processes 3–5 μm (mean 3 μm, N = 2); ~25–52 processes on vesicle periphery in circumferential view.

Material.—One specimen from Unit 4A of the Ediacaran Doushantuo Formation in the Weng'an area.

Remarks.—The specimen exhibits similarities to *Weissiella grandistella* in terms of process morphology, length, and crosswalls. However, its vesicle diameter is smaller compared to that reported for *W. grandistella* specimens from the East European Platform (vesicle diameter 450–500 μm). Following the description of *W.* cf. *W. grandistella* by Ouyang et al.

https://doi.org/10.1017/jpa.2024.16 Published online by Cambridge University Press

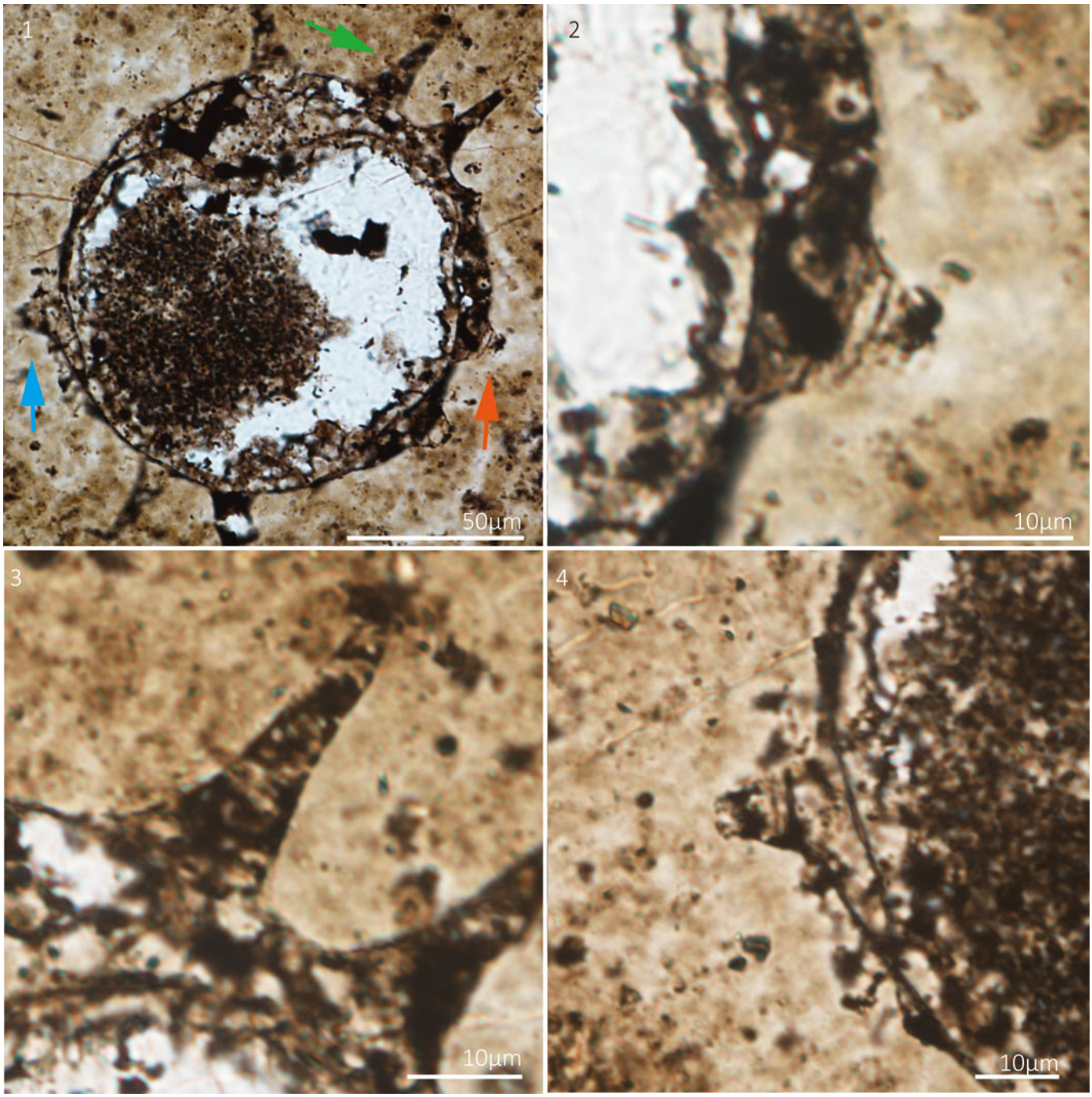

Figure 10. *Weissiella* cf. *W. grandistella* Vorob'eva, Sergeev, and Knoll, 2009, emend. Liu and Moczydłowska, 2019. Thin section numbers: (**1**) WS17-2-195-X54Y101. (**2–4**) Magnified views of (**1**) showing crosswall structures: (**2**) red arrow; (**3**) green arrow; (**4**) blue arrow.

(2021) and Ye at al. (2022), we categorize our specimen as *W.* cf. *W. grandistella.*

Summary of taxonomy

After examining >500 thin sections of black phosphorite, we discovered numerous acanthomorphic acritarchs, the majority of which belong to LAAs with a diameters > 200 μm. Although we identified several new species of *Yinitianzhushania* that might have not been reported previously (which will be discussed in a separate paper), most of the specimens can be attributed to previously reported genera. This report specifically delves into SAAs, particularly those with diameters <60 μm (Fig. 11). These diminutive specimens have been infrequently reported by previous researchers in the Weng'an Biota. The abundance of these SAAs is significantly lower than that of LAAs. Due to their smaller size, they are more difficult to detect under the microscope. We discovered >70 specimens of SAAs (< 60 μm in diameter; Fig. 11) and three specimens of MAAs (no more than 150 μm in diameter; Fig. 11).

https://doi.org/10.1017/jpa.2024.16 Published online by Cambridge University Press

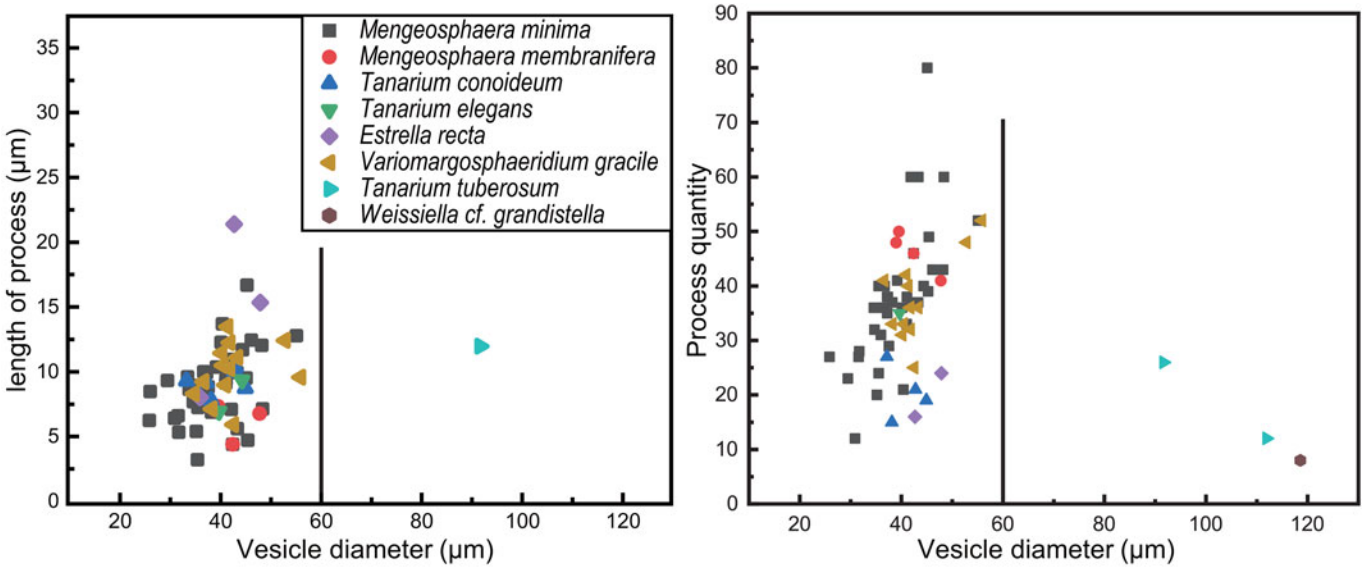

Figure 11. Measurements for process length (left) and process quantity (right) versus vesicle diameter of acanthomorphic acritarchs in the Weng'an Biota.

Based on detailed observations and microscopic imaging (Fig. 12), we characterized the vesicle morphology and structure of these small and medium-sized acritarchs, including the shape, length, and density of their processes (specific descriptions are in the Systematic paleontology section). Through meticulous morphological comparison, we preliminarily identified seven species from four genera, namely *Tanarium conoideum*, *Tanarium elegans*, *Tanarium tuberosum*, *Mengeosphaera membranifera*, *M. minima*, *Estrella recta*, and *Variomargosphaeridium gracile*, and one possibly new form tentatively placed in open nomenclature, *Weissiella* cf. *W. grandistella*. The abundance of *Mengeosphaera* and *Tanarium* specimens was relatively higher, accounting for > 60% of the discovered specimens, whereas the abundance of the other taxa was relatively low. *Mengeosphaera* was identified by its biform process, whereas *Tanarium* was identified by its conical process; *Estrella* by the length of its processes exceeding the vesicle diameter; *Variomargosphaeridium* by branching hollow processes; and *Weissiella* by short conical to cylindrical processes with internal crosswalls.

Tanarium conoideum was previously reported in the Weng'an Biota by an earlier study (Xiao et al., 2014a). However, the specimens that they reported had a diameter >100 μm, whereas the specimens that we reported for the same species had a diameter of no more than 60 μm. The other SAAs and MAAs from three genera and five species (*Estrella recta, Mengeosphaera membranifera*, *Mengeosphaera minima*, *Tanarium elegans*, and *Tanarium tuberosum*) mentioned above were discovered for the first time in the Weng'an Biota. These fossils not only provide new materials for reconstructing the composition of the fossil assemblage of the Weng'an Biota, but also offer new evidence for gaining a more comprehensive understanding of the marine ecosystem at that time.

Moreover, these SAAs are not exclusive to the Weng'an Biota. Some common acritarch elements have also been found in the Yangtze Gorges region of South China, Australia, Siberia, and the East European Platform (Fig. 12). For example, *Estrella recta* and *Mengeosphaera bellula* were found in both the Weng'an and the Yangtze Gorges region of South China, whereas *Tanarium tuberosum* was found in the Weng'an and the Yangtze Gorges region of South China, the Easten Officer Basin of South Australia, the Siberian Platform of Russia, and the Timan Ridge of the East European Platform. *Tanarium conoideum* was found in the Weng'an, the Yangtze Gorges of South China, and the Siberia Platform of Russia. Although their phylogenetic affinities are still disputed, these globally distributed acanthomorphic acritarchs have the potential to be further explored in the subdivision and global/regional correlation of the Ediacaran system.

Implications for biostratigraphic correlation

Given the widespread distribution of these newly discovered acanthomorphic acritarchs in the Weng'an Biota, they have the potential to contribute to stratigraphic division and correlation within the Ediacaran System. In 2014, Liu et al. established two biozones based on acritarch fossil assemblages from the Ediacaran Doushantuo Formation in the Yangtze Gorges area: the lower acritarch biozone, dominated by *Tianzhushania spinosa* Yin and Li, 1978, emend. C. Yin in Yin and Liu, 1988, and the upper acritarch biozone, dominated by *Tanarium conoideum*, *Hocosphaeridium scaberfacium* Zhang in Zhang and Walter, 1992, and *Hocosphaeridium anozos* (see Liu et al., 2014a). Liu and Moczydłowska (2019) proposed four new biozones based on the latest fossil data, in ascending order: the *Appendisphaera grandis-Weissiella grandistella-Tianzhushania spinosa* Assemblage Zone, *Tanarium tuberosum-Schizofusa zangwenlongii* Assemblage Zone, *Tanarium conoideum-Cavaspina basiconica* Assemblage Zone, and *Tanarium pycnacanthum-Ceratosphaeridium glaberosum* Assemblage Zone.

Among the newly discovered SAAs and MAAs in the Weng'an Biota, *Tanarium tuberosum* from the Yangtze Gorges area belongs to the *Tanarium tuberosum-Schizofusa zangwenlongii* Assemblage Zone, whereas *Tanarium conoideum* comes from the *Tanarium conoideum-Cavaspina basiconica* Assemblage

https://doi.org/10.1017/jpa.2024.16 Published online by Cambridge University Press

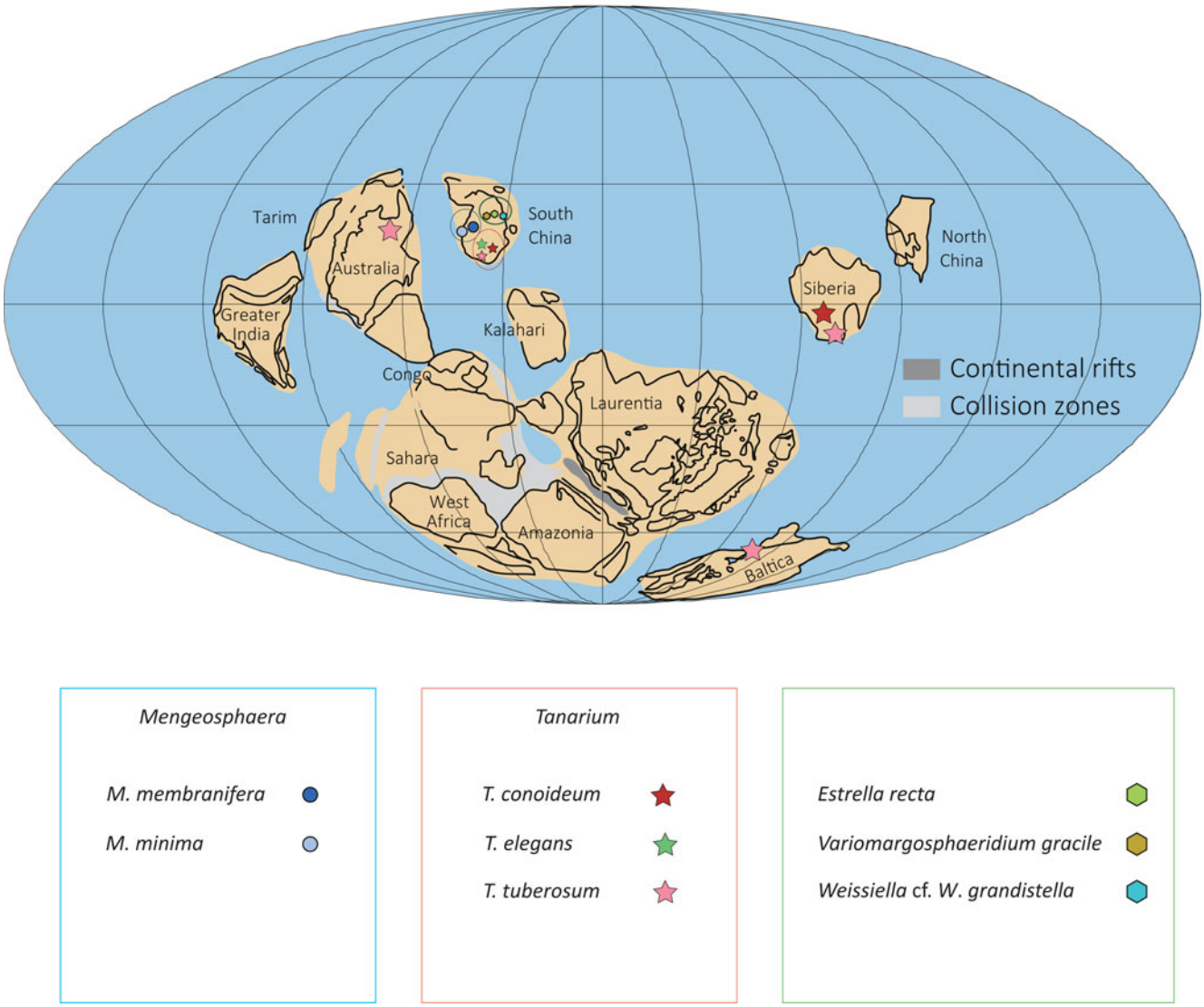

Figure 12. The distribution of the Ediacaran small and medium-sized acanthomorphic acritarchs in the present study (modified from Li et al., 2008).

Zone. Considering the presence of *Tianzhushania spinosa* in the Weng'an Biota, it belongs to the *Appendisphaera grandis-Weissiella grandistella-Tianzhushania spinosa* Assemblage Zone in the Yangtze Gorges area. In the Doushantuo Formation of the Weng'an area, these taxa mainly come from a < 2 m thick layer of black phosphorite (Unit 4A). This contrasts with the Yangtze Gorges area, where the distribution ranges of acritarchs in the four biozones do not overlap. This situation poses challenges for stratigraphic correlation.

The acritarch fossil assemblage from the Weng'an Biota, as presented in this report, originates from the same stratigraphic horizon, namely Unit 4A of the Doushantuo Formation in the Weng'an area. However, the acritarch fossils of the same genus and species in the Yangtze Gorges area are distributed across three different fossil zones within Member II of the Doushantuo Formation. Several factors could contribute to this discrepancy. We believe that the 2 m thick black phosphorite (Unit 4A) is highly condensed, and the fossils in the Weng'an Biota are not in situ but rather redeposited after undergoing repeated transportation and reworking within the basin (Yin et al., 2014; Bottjer et al., 2020). This might explain why acritarchs that were originally expected to come from three different fossil zones (i.e., different stratigraphic layers) coexist in one 2 m thick stratigraphic layer in the Weng'an area's Doushantuo Formation. Despite this, previous studies have reported 24 genera and 69 species of acritarchs from Member Ⅱ of the Doushantuo Formation at three sections (Jiulongwan, Jinguadun, and Wuzhishan) in the Yangtze Gorges area (Ouyang et al., 2021). Two taxa (*Mengeosphaera minima* and *Weissiella* cf. *W. grandistella*) in this study are consistent with those reported by Ouyang et al. (2021). It is recommended to correlate Unit 4A of the Doushantuo Formation containing the Weng'an Biota to the Ediacaran Doushantuo Formation Member Ⅱ in the Yangtze Gorges area using acritarch fossils (Xiao et al., 2014a; Liu and Moczydłowska, 2019; Ouyang et al., 2019).

https://doi.org/10.1017/jpa.2024.16 Published online by Cambridge University Press

In 2005, Grey identified the *Tanarium conoideum-Schizofusa risoria-Variomargosphaeridium litoschum* Assemblage Zone in the Australian Ediacaran strata. Some acritarch species from this biozone have also been found in the Weng'an area, including *Tanarium conoideum* and *Variomargosphaeridium litoschum*. Consequently, Xiao et al. (2014a) suggested correlating the stratigraphic level of the Weng'an Biota to the *Tanarium conoideum-Schizofusa risoria-Variomargosphaeridium litoschum* Assemblage Zone in the Australian Ediacaran System. The new findings in this study are consistent with this perspective. However, considering the co-occurrence of acritarch fossils from different biozones in the same black phosphorite horizon (i.e., Unit 4A of the Doushantuo Formation) in the Weng'an area, it is challenging to separate their distribution ranges in the stratigraphic sequence, and such correlations should be made cautiously. In the future, conducting higher-resolution stratigraphic sampling of acanthomorphic acritarch fossils in the black phosphorite and gray phosphatic dolomite of the Weng'an Doushantuo Formation could contribute to a more comprehensive resolution of this issue.

Conclusion

This study discovered seven species and one possible new form tentatively placed in open nomenclature (*Weissiella* cf. *W. grandistella*) of SAAs and MAAs in the Weng'an Biota, including five species reported for the first time in the Weng'an area. Together with the previously reported fossil materials, there are a total of 50 species and one undetermined species of acanthomorphs in the Weng'an Biota (Table 1). Although some of these acritarchs are local species, most of these species have also been found in other regions, e.g., the Yangtze Gorges area (South China), Australia, and Siberia. The presence of so many shared acritarch species among different regions plays a crucial role in the subdivision and correlation of the Ediacaran System. Based on the current data, the acritarch assemblages of the Doushantuo Formation in the Weng'an area share common species with three acritarch assemblage zones (*Appendisphaera grandis–Weissiella grandistella–Tianzhushania spinosa* Assemblage Zone, *Tanarium tuberosum–Schizofusa zangwenlongii* Assemblage Zone, and *Tanarium conoideum–Cavaspina basiconica* Assemblage Zone) from the lower part of Member II of the Ediacaran Doushantuo Formation in the Yangtze Gorges area, as well as the *Tanarium conoideum–Schizofusa risoria–Variomargosphaeridium litoschum* Assemblage Zone from the Ediacaran Pertatataka Formationin in Australia. This taxonomic similarity indicates a correlation of Unit 4A of the Ediacaran Doushantuo Formation in the Weng'an area, Member II of the Ediacaran Doushantuo Formation in the Yangtze Gorges area, and the upper part of the Ediacaran Pertatataka Formation in Australia.

The fossils reported in this report were collected from the black phosphorites of the Doushantuo Formation in Weng'an. Similar to the chert nodules in the Yangtze Gorges area, the study of acritarchs in black phosphorites can only be conducted through thin sections. Because the information obtained from acritarchs observed in thin sections differs to some extent from the compressed organic acritarchs obtained from shale through acid maceration, achieving consistent taxonomic criteria for acritarchs from different taphonomic windows becomes challenging. This inconsistency somewhat undermines the potential of acritarchs in biostratigraphic subdivision and correlation. Therefore, achieving higher-resolution biostratigraphic correlation of the Ediacaran System in the future not only requires detailed layer-by-layer sampling in different localities, but also needs to overcome the preservation bias and inconsistency in taxonomic criteria for acritarchs from different taphonomic windows by introducing new techniques and methods.

Acknowledgments

This work was supported by the National Natural Science Foundation of China (42022010, 41921002, U2244202). We would like to thank Professor C. Zhou for providing suggestions about schematic drawings, and we thank the guest editor T. Selly. We are also most grateful for the detailed and constructive comments provided by two anonymous referees.

Declaration of competing interests

The authors declare none.

References

Anderson, R.P., Macdonald, F.A., Jones, D.S., McMahon, S., and Briggs, D.E.G., 2017, Doushantuo-type microfossils from latest Ediacaran phosphorites of northern Mongolia: Geology, v. 45, no. 12, p. 1079–1082, https://doi.org/10.1130/G39576.1.

Bottjer, D.J., Yin, Z.J., Zhao, F.C., and Zhu, M.Y., 2020, Comparative taphonomy and phylogenetic signal of phosphatized Weng'an and Kuanchuanpu Biotas: Precambrian Research, v. 349, n. 105408, https://doi.org/10.1016/j.precamres.2019.105408.

Chen, J.Y., 2004, The Dawn of Animal World: Nanjing, China, Jiangsu Science and Technology Press, 336 p.

Chen, M.E., and Liu, K.W., 1986, The geological significance of newly discovered microfossils from the upper Sinian (Doushantuo age) phosphorites: Scientia Geologica Sinica, v. 1, p. 46–53.

Chen, S., Yin, C., Liu, P., Gao, L., Tang, F., and Wang, Z., 2010, Microfossil assemblage from chert nodules of the Ediacaran Doushantuo Formation in Zhangcunping, northern Yichang, South China: Acta Geologica Sinica (Chinese Edition), v. 84, p. 70–77. [In Chinese]

Condon, D., Zhu, M., Bowring, S., Wang, W., Yang, A., and Jin, Y., 2005, U-Pb ages from the neoproterozoic Doushantuo Formation, China: Science, v. 308, no. 5718, p. 95–98, https://doi.org/10.1126/science.1107765.

Cunningham, J., Vargas, K., Yin, Z., Bengtson, S., and Donoghue, P., 2017, The Weng'an biota (Doushantuo Formation): an Ediacaran window on soft-bodied and multicellular microorganisms: Journal of the Geological Society, v. 174, no. 5, p. 793–802, https://doi.org/10.1144/jgs2016-142.

Evitt, W.R., 1963, A discussion and proposals concerning fossil dinoflagellates, hystrichospheres, and acritarchs: Proceedings of the National Academy of Sciences of the United States of America, v. 49, p. 158–164, 298–302.

Golubkova, E.Y., Raevskaya, E.G., and Kuznetsov, A.B., 2010, Lower Vendian microfossil assemblages of East Siberia: significance for solving regional stratigraphic problems: Stratigraphy and Geological Correlation, v. 18, no. 4, p. 353–375, https://doi.org/10.1134/S0869593810040015.

Grey, K., 2005, Ediacaran Palynology of Australia: Canberra, Association of Australasian Palaeontologists, Memoir 31, 439 p.

Knoll, A.H., 1984, Microbiotas of the late Precambrian Hunnberg Formation, Nordaustlandet, Svalbard: Journal of Paleontology, v. 58, p. 131–162.

Knoll, A., 1992, Microfossils in metasedimentary cherts of the Scotia Group, Prins Karls Forland, western Svalbard: Palaeontology, v. 35, p. 751–774.

https://doi.org/10.1017/jpa.2024.16 Published online by Cambridge University Press

Knoll, A.H., Swett, K., and Mark, J., 1991, Paleobiology of a Neoproterozoic tidal flat/lagoonal complex: the Draken Conglomerate Formation, Spitsbergen: Journal of Paleontology, v. 65, no. 4, p. 531–570.
Kolosova, S.P., 1991, Late Precambrian spiny microfossils from the eastern part of the Siberian Platform: Algologiya, v. 1, no. 2, p. 53–59.
Li, Z.X., Bogdanova, S.V., Collins, A.S., Davidson, A., Waele, B., Ernst, R.E., Fitzsimons, I.C.W., Fuck, R.A., Gladkochub, D.P., Jacobs, J., Karlstrom, K.E., Lu, S., Natapov, L.M., Pease, V., Pisarevsky, S.A., Thrane, K., and Vernikovsky, V., 2008, Assembly, configuration, and break-up history of Rodinia: a synthesis: Precambrian Research, v. 160, p. 179–210, https://doi.org/10.1016/j.precamres.2007.04.021.
Liu, P., and Moczydłowska, M., 2019, Ediacaran microfossils from the Doushantuo Formation chert nodules in the Yangtze Gorges area, South China, and new biozones: Fossils and Strata, v. 65, p. 1–172, https://doi.org/10.1002/9781119564225.ch1.
Liu, P., and Yin, C., 2005, New data of phosphatized acritarchs from the Ediacaran Doushantuo Formation at Weng'an, Guizhou Province, southwest China: Acta Geologica Sinica (English Edition), v. 79, p. 575–581.
Liu, P., Yin, C., Chen, S., Tang, F., and Gao, L., 2012, Discovery of Ceratosphaeridium (Acritarcha) from the Ediacaran Doushantuo Formation in Yangtze Gorges, South China and its biostratigraphic implication: Bulletin of Geosciences, v. 87, p. 195–200, https://doi.org/10.3140/bull.geosci.1223.
Liu, P., Xiao, S., Yin, C., Chen, S., Zhou, C., and Li, M., 2014a, Ediacaran acanthomorphic acritarchs and other microfossils from chert nodules of the upper Doushantuo Formation in the Yangtze Gorges area, South China: Journal of Paleontology, v. 88, no. 1, p. 1–139, https://doi.org/10.1666/13-009.
Liu, P., Chen, S., Zhu, M., Li, M., Yin, C., and Shang, X., 2014b, High-resolution biostratigraphic and chemostratigraphic data from the Chenjiayuanzi section of the Doushantuo Formation in the Yangtze Gorges area, South China: implication for subdivision and global correlation of the Ediacaran System: Precambrian Research, v. 249, p. 199–214, https://doi.org/10.1016/j.precamres.2014.05.014.
McFadden, K., Xiao, S., Zhou, C., and Kowalewski, M., 2009, Quantitative evaluation of the biostratigraphic distribution of acanthomorphic acritarchs in the Ediacaran Doushantuo Formation in the Yangtze Gorges area, South China: Precambrian Research, v. 173, nos. 1–4, p. 170–190, https://doi.org/10.1016/j.precamres.2009.03.009.
Moczydłowska, M., 2005, Taxonomic review of some Ediacaran acritarchs from the Siberian Platform: Precambrian Research, v. 136, no. 3/4, p. 283–307, https://doi.org/10.1016/j.precamres.2004.12.001.
Moczydłowska, M., 2015, Algal affinities of Ediacaran and Cambrian organic-walled microfossils with internal reproductive bodies: *Tanarium* and other morphotypes: Palynology, v. 40, no. 1, p. 83–121, https://doi.org/10.1080/01916122.2015.1006341.
Moczydłowska, M., and Nagovitsin, K., 2012, Ediacaran radiation of organic-walled microbiota recorded in the Ura Formation, Patom Uplift, East Siberia: Precambrian Research, v. 198–199, p. 1–24, https://doi.org/10.1016/j.precamres.2011.12.010.
Moczydłowska, M., Vidal, G., and Rudavskaya, V., 1993, Neoproterozoic (Vendian) phytoplankton from the Siberian Platform, Yakutia: Palaeontology, v. 36, no. 3, p. 495–521.
Nagovitsyn, K.E., Faizullin, M.S., and Yakshin, M.S., 2004, New forms of Baikalian acanthomorphytes from the Ura Formation of the Patom Uplift, East Siberia: Geologiya e Geofisika, v. 45, p. 7–19.
Narbonne, G., Xiao, S., and Shields, G., 2012, The Ediacaran Period, *in* Gradstein, F.M., Ogg, J.G., Schmitz, M.D., et al., eds., The Geologic Time Scale 2012: Boston, Elsevier, p. 413–435.
Ouyang, Q., Zhou, C., Xiao, S., Chen, Z., and Shao, Y., 2019, Acanthomorphic acritarchs from the Ediacaran Doushantuo Formation at Zhangcunping in South China, with implications for the evolution of early Ediacaran eukaryotes: Precambrian Research, v. 320, p. 171–192, https://doi.org/10.1016/j.precamres.2018.10.012.
Ouyang, Q., Zhou, C., Xiao, S., Guan, C., Chen, Z., Yuan, X., and Sun, Y., 2021, Distribution of Ediacaran acanthomorphic acritarchs in the lower Doushantuo Formation of the Yangtze Gorges area, South China: evolutionary and stratigraphic implications: Precambrian Research, v. 353, n. 106005, https://doi.org/10.1016/j.precamres.2020.106005.
Prasad, B., and Ramson, A., 2016, Record of Ediacaran complex acanthomorphic acritarchs from the lower Vindhyan succession of the Chambal Valley (East Rajasthan), India and their biostratigraphic significance: Journal of the Palaeontological Society of India, v. 61, p. 29–62.
Sergeev, V., Knoll, A., and Vorob'eva, N., 2011, Ediacaran microfossils from the Ura Formation, Baikal-Patom Uplift, Siberia: taxonomy and biostratigraphic significance: Journal of Paleontology, v. 85, no. 5, p. 987–1011, https://doi.org/10.1666/11-022.1.
Shang, X., Liu, P., and Moczydłowska, M., 2019, Acritarchs from the Doushantuo Formation at Liujing section in Songlin area of Guizhou Province, South China: implications for early–middle Ediacaran biostratigraphy: Precambrian Research, v. 334, n. 105453, https://doi.org/10.1016/j.precamres.2019.105453.
Steiner, M., Li, G., Qian, Y., Zhu, M., and Erdtmann, B.D., 2007, Neoproterozoic to early Cambrian small shelly fossil assemblages and a revised biostratigraphic correlation of the Yangtze Platform (China): Palaeogeography, Palaeoclimatology, Palaeoecology, v. 254, no. 1/2, p. 67–99, https://doi.org/10.1016/j.palaeo.2007.03.046.
Veis, A.F., Vorob'eva, N.G., and Goubkova, E.Y., 2006, The early Vendian microfossils first found in the Russian Plate: taxonomic composition and biostratigraphic significance: Stratigraphy and Geological Correlation, v. 14, p. 368–385, https://doi.org/10.1134/S0869593806040022.
Vidal, G., 1990, Giant acanthomorph acritarchs from the upper Proterozoic in southern Norway: Palaeontology, v. 33, p. 287–298.
Vorob'eva, N.G., and Petrov, P.Y., 2020, Microbiota of the Barakun Formation and biostratigraphic characteristics of the Dal'nyaya Taiga Group: early Vendian of the Ura Uplift (eastern Siberia): Stratigraphy and Geological Correlation, v. 28, p. 365–380, https://doi.org/10.1134/S0869593820040103.
Vorob'eva, N.G., Sergeev, V.N., and Chumakov, N.M., 2008, New finds of early Vendian microfossils in the Ura Formation: revision of the Patom Supergroup Age, middle Siberia: Doklady Earth Sciences, v. 419, no. A, p. 411–416, https://doi.org/10.1134/S1028334X08030136.
Vorob'eva, N.G., Sergeev, V.N., and Knoll, A.H., 2009, Neoproterozoic microfossils from the northeastern margin of the East European Platform: Journal of Paleontology, v. 83, no. 2, p. 161–196, https://doi.org/10.1666/08-064.1.
Willman, S., and Moczydłowska, M., 2008, Ediacaran acritarch biota from the Giles 1 drillhole, Officer Basin, Australia, and its potential for biostratigraphic correlation: Precambrian Research, v. 162, no. 3/4, p. 498–530, https://doi.org/10.1016/j.precamres.2007.10.010.
Willman, S., and Moczydłowska, M., 2011, Acritarchs in the Ediacaran of Australia—local or global significance? Evidence from the Lake Maurice West 1 drillcore: Review of Palaeobotany and Palynology, v. 166, no. 1/2, p. 12–28, https://doi.org/10.1016/j.revpalbo.2011.04.005.
Willman, S., Moczydłowska, M., and Grey, K., 2006, Neoproterozoic (Ediacaran) diversification of acritarchs—a new record from the Murnaroo 1 drillcore, eastern Officer Basin, Australia: Review of Palaeobotany and Palynology, v. 139, no. 1–4, p. 17–39, https://doi.org/10.1016/j.revpalbo.2005.07.014.
Xiao, S., 2004, New multicellular algal fossils and acritarchs in Doushantuo chert nodules (Neoproterozoic, Yangtze Gorges, South China): Journal of Paleontology, v. 78, p. 393–401, https://doi.org/10.1666/0022-3360(2004)078<0393:NMAFAA>2.0.CO;2.
Xiao, S., and Knoll, A., 1999, Fossil preservation in the Neoproterozoic Doushantuo phosphorite Lagerstätte, South China: Lethaia, v. 32, p. 219–240.
Xiao, S., and Knoll, A., 2000, Phosphatized animal embryos from the Neoproterozoic Doushantuo Formation at Weng'an, Guizhou, South China: Journal of Paleontology, v. 74, no. 5, p. 767–788, https://doi.org/10.1666/0022-3360(2000)074<0767:PAEFTN>2.0.CO;2.
Xiao, S., and Knoll, A.H., 2007, Fossil preservation in the Neoproterozoic Doushantuo phosphorite Lagerstatte, South China: Lethaia, v. 32, p. 219–238, https://doi.org/10.1111/j.1502-3931.1999.tb00541.x.
Xiao, S., and Narbonne, G., 2020, The Ediacaran Period in geologic time, *in* Gradstein, F.M., Ogg, J.G., Schmitz, M.D., and Ogg, G.M., eds., The Geologic Time Scale 2020: Boston, Elsevier, p. 521–561.
Xiao, S., Zhang, Y., and Knoll, A., 1998, Three-dimensional preservation of algae and animal embryos in a Neoproterozoic phosphorite: Nature, v. 391, no. 6667, p. 553–558.
Xiao, S., Knoll, A., Zhang, L., and Hua, H., 1999, The discovery of *Wengania globosa* in Doushantuo phosphorites in Chadian, Shaanxi Province: Acta Micropalaeontologica Sinica, v. 16, p. 259–266.
Xiao, S., Schiffbauer, J., McFadden, K., and Hunter, J., 2010, Petrographic and SIMS pyrite sulfur isotope analyses of Ediacaran chert nodules: implications for microbial processes in pyrite rim formation, silicification, and exceptional fossil preservation: Earth and Planetary Science Letters, v. 297, no. 3/4, p. 481–495, https://doi.org/10.1016/j.epsl.2010.07.001.
Xiao, S., Zhou, C., Liu, P., Wang, D., and Yuan, X., 2014a, Phosphatized acanthomorphic acritarchs and related microfossils from the Ediacaran Doushantuo Formation at Weng'an (South China) and their implications for biostratigraphic correlation: Journal of Paleontology, v. 88, no. 1, p. 1–67, https://doi.org/10.1666/12-157R.
Xiao, S., Muscente, A., Chen, L., Zhou, C., Schiffbauer, J., Wood, A., Polys, N., and Yuan, X., 2014b, The Weng'an biota and the Ediacaran radiation of multicellular eukaryotes: National Science Review, v. 1, no. 4, p. 498–520, https://doi.org/10.1093/nsr/nwu061.
Xie, G., Zhou, C., Mcfadden, K.A., Xiao, S., and Yuan, X., 2008, Microfossils discovered from the Sinian Doushantuo Formation in the Jiulongwan section, East Yangtze Gorges area, Hubei Province, South China: Acta Palaeontologica Sinica, v. 47, p. 279–291.

https://doi.org/10.1017/jpa.2024.16 Published online by Cambridge University Press

Yang, L., Pang, K., Chen, L., Zhong, Z., and Yang, F., 2020, New materials of microfossils from the Ediacaran Doushantuo Formation in Baizhu phosphorite deposit, Baokang, Hubei Provience [sic]: Acta Micropalaeontologica Sinica, v. 37, no. 1, p. 1–20.
Yang, C., Rooney, A., Condon, D., Li, X., Grazhdankin, D., Bowyer, F., Hu, C., Macdonald, F.A., and Zhu, M., 2021, The tempo of Ediacaran evolution: Science Adances, v. 7, no. 45, n. 9643, https://doi.org/10.1126/sciadv.abi9643.
Ye, Q., Li, J., Tong, J., An, Z., Hu, J., and Xiao, S., 2022, A microfossil assemblage from the Ediacaran Doushantuo Formation in the Shennongjia area (Hubei Province, South China): filling critical paleoenvironmental and biostratigraphic gaps: Precambrian Research, v. 377, n. 106691, https://doi.org/10.1016/j.precamres.2022.106691.
Yin, C., 1990, Spinose acritarchs from the Toushantuo Formation and its geological significance: Acta Micropalaeontologica Sinica, v. 7, p. 265–270.
Yin, C., and Liu, G., 1988, Micropaleofloras, *in* Zhao, Z., Xing, Y., Ding, Q., Liu, G., Zhao, Y., et al., eds., The Sinian System of Hubei: Wuhan, China University of Geosciences Press, p. 170–180.
Yin, C., Liu, P., Awramik, S.M., Chen, S., Tang, F., Gao, L., Wang, Z., and Riedman, L.A., 2011, Acanthomorph biostratigraphic succession of the Ediacaran Doushantuo Formation in the East Yangtze Gorges, South China: Acta Geologica Sinica (English Edition), v. 85, p. 283–295, https://doi.org/10.1111/j.1755-6724.2011.00398.x.
Yin, L., 1987, Microbiotas of latest Precambrian sequences in China, *in* Nanjing Institute of Geology and Palaeontology Academica Sinica, ed., Stratigraphy and Palaeontology of Systemic Boundaries in China: Precambrian-Cambrian Boundary (1): Nanjing, China, Nanjing University Press, p. 415– 494.
Yin, L., and Li, Z., 1978, Precambrian microfloras of southwest China with reference to their stratigraphic significance: Memoir, Nanjing Institute of Geology and Palaeontology, Academia Sinica, v. 10, p. 41–108.
Yin, L., Zhu, M., Knoll, A., Yuan, X., Zhang, J. and Hu, J., 2007, Doushantuo embryos preserved inside diapause egg cysts: Nature, v. 446, p. 661–663, https://doi.org/10.1038/nature05682.
Yin, L., Zhou, C., and Yuan, X., 2008, New data on *Tianzhushania*—an Ediacaran diapause egg cyst from Yichang, Hubei: Acta Palaeontologica Sinica, v. 47, p. 129–140.
Yin, L., Wang, D., Yuan, X., and Zhou, C., 2011, Diverse small spinose acritarchs from the Ediacaran Doushantuo Formation, South China: Palaeoworld, v. 20, no. 4, p. 279–289, https://doi.org/10.1016/j.palwor.2011.10.002.
Yin, Z., Zhu, M., Tafforeau, P., Chen, J., Liu, P., and Li, G., 2013, Early embryogenesis of potential bilaterian animals with polar lobe formation from the Ediacaran Weng'an Biota, South China: Precambrian Research, v. 225, p. 44–57, https://doi.org/10.1016/j.precamres.2011.08.011.
Yin, Z., Liu, P., Li, G., Tafforeau, P., and Zhu, M., 2014, Biological and taphonomic implications of Ediacaran fossil embryos undergoing cytokinesis: Gondwana Research, v. 25, no. 3, p. 1019–1026, https://doi.org/10.1016/j.gr.2013.01.008.
Yin, Z., Zhu, M., Davidson, E.H., Bottjer, D.J., Zhao, F., and Tafforeau, P., 2015, Sponge grade body fossil with cellular resolution dating 60 Myr before the Cambrian: Proceedings of the National Academy of Sciences, v. 112, no. 12, p. E1453–E1460, https://doi.org/10.1073/pnas.1414577112.
Yuan, X., and Hofmann, H.J., 1998, New microfossils from the Neoproterozoic (Sinian) Doushantuo Formation, Weng'an, Guizhou Province, southwestern China: Alcheringa, v. 22, p. 189–222.
Yuan, X., Xiao, S., Yin, L., Knoll, A., Zhou, C., and Mu, X., 2002, Doushantuo Fossils: Life on the Eve of Animal Radiation: Hefei, China, China University of Science and Technology Press, 171 p. [In Chinese, with English summary]
Zang, W., and Walter, M.R., 1992, Late Proterozoic and Cambrian microfossils and biostratigraphy, Amadeus Basin, central Australia: The Association of Australasia Palaeontologists Memoir, v. 12, p. 1–132.
Zhang, Y., Yin, L., Xiao, S., and Knoll, A., 1998, Permineralized fossils from the terminal Proterozoic Doushantuo Formation, South China: Journal of Paleontology Memoir, v. 72, supplement, p. 1–52.
Zhou, C., Brasier, M., and Xue, Y., 2001, Three-dimensional phosphatic preservation of giant acritarchs from the terminal Proterozoic Doushantuo Formation in Guizhou and Hubei provinces, South China: Palaeontology, v. 44, p. 1157–1178, https://doi.org/10.1111/1475-4983.00219.
Zhou, C., Chen, Z., and Xue, Y., 2002a, New microfossils from the late Neoproterozoic Doushantuo Formation at Chaoyang phosphorite deposit in Jiangxi Province, South China: Acta Palaeontologica Sinica, v. 41, p. 178–192.
Zhou, C., Yuan, X., and Xiao, S., 2002b, Phosphatized biotas from the Neoproterozoic Doushantuo Formation on the Yangtze Platform: Chinese Science Bulletin, v. 47, p. 1918–1924, https://doi.org/10.1360/02tb9419.
Zhou, C., Yuan, X., Xiao, S., Chen, Z., and Xue, Y., 2004, Phosphatized fossil assemblage from the Doushantuo Formation in Baokang, Hubei Province: Acta Micropalaeontologica Sinica, v. 21, p. 349–366.
Zhou, C., Xie, G., Mcfadden, K., Xiao, S., and Yuan, X., 2007, The diversification and extinction of Doushantuo-Pertatataka acritarchs in South China: causes and biostratigraphic significance: Geological Journal, v. 42, p. 229–262, https://doi.org/10.1002/gj.1062.
Zhou, C., Li, X.-H., Xiao, S., Lan, Z., Ouyang, Q., Guan, C., and Chen, Z., 2017, A new SIMS zircon U-Pb date from the Ediacaran Doushantuo Formation: age constraint on the Weng'an biota: Geological Magazine, v. 154, no. 6, p. 1193–1201, https://doi.org/10.1017/S0016756816001175.
Zhou, C., Yuan, X., Xiao, S., Chen, Z., and Hua, H., 2019, Ediacaran integrative stratigraphy and timescale of China: Science China-Earth Sciences, v. 62, no. 1, p. 7–24, https://doi.org/10.1007/s11430-017-9216-2.
Zhu, M., Zhang, J., and Yang, A., 2007, Integrated Ediacaran (Sinian) chronostratigraphy of South China: Palaeogeography, Palaeoclimatology, Palaeoecology, v. 254, no. 1/2, p. 7–61, https://doi.org/10.1016/j.palaeo/2007.03.025.
Zhu, M., Lu, M., Zhang, J., Zhao, F., Li, G., Aihua, Y., Zhao, X., and Zhao, M., 2013, Carbon isotope chemostratigraphy and sedimentary facies evolution of the Ediacaran Doushantuo Formation in western Hubei, South China: Precambrian Research, v. 225, p. 7–28, https://doi.org/10.1016/j.precamres.2011.07.019.
Zhu, M., Yang, A., Yuan, J., Li, G., Zhang, J., Zhao, F., Ahn, S., and Miao, L., 2019, Cambrian integrative stratigraphy and timescale of China: Science China Earth Sciences, v. 62, p. 25–60, https://doi.org/10.1007/s11430-017-9291-0.

https://doi.org/10.1017/jpa.2024.16 Published online by Cambridge University Press

Appendix 1. Measured data of acritarchs in this study.

Taxon	Thin section no.	Vesicle diameter (μm)	Length of processes (mean μm/N)	Distance between processes (mean μm/N)	Basal width of process (mean μm/N)	Quantity of processes
Mengeosphaera minima Liu et al., 2014a	WS17-2-193-X46Y104	40	mean 13/N 21	mean 6/N 5	mean 4/N 10	21
	WS17-3-219-X25Y101	41	mean 9/N 38	mean 4/N 7	mean 3/N 6	38
	WS17-3-220-X38Y100	39	mean 10/N 41	mean 4/N 7	mean 3/N 8	41
	WS17-3-224-X45Y110	46	mean 12/N 43	mean 4/N 8	mean 3/N 9	43
	WS17-3-235-X59Y107	40	mean 12/N 36	mean 4/N 5	mean 3/N 5	36
	WS17-3-256-X36Y114	37	mean 10/N 40	mean 4/N 7	mean 3/N 7	40
	WS17-2-145-X50Y98	45	mean 17/N 39	mean 4/N 4	mean 3/N 6	39
	WS17-2-153-X31Y91	38	mean 9/N 29	mean 4/N 8	mean 3/N 7	29
	WS17-3-217-X48Y101	43	mean 10/N 37	mean 4/N 9	mean 4/N 6	37
	WS17-3-227-X46Y99	35	mean 7/N 24	mean 5/N 6	mean 3/N 7	~24
	WS17-3-227-X55Y97	35	mean 10/N 40	mean 4/N 7	mean 2/N 5	~40
	WS17-3-231-X58Y112	42	mean 7/N 37	mean 4/N 7	mean 3/N 8	37
	WS17-2-159-X26Y115	none	mean 5/N 40	mean 3/N 10	mean 2/N 8	40
	WS17-2-164-X38Y98	55	mean 13/N 52	mean 4/N 7	mean 3/N 6	52
	WS17-3-207-X17Y99	37	mean 10/N 38	mean 5/N 6	mean 3/N 6	38
	WS17-3-208-X35Y105	44	mean 12/N 40	mean 5/N 6	mean 3/N 5	~40
	WS17-2-145-X41.5Y115	33	10/N 1	none	mean 2/N 4	none
	WS17-2-150-X47Y108	35	mean 5/N 30	mean 3/N 5	mean 2/N 4	~60
	WS17-2-164-X44Y104	43	11/N 1	none	none	none
	WS17-3-211-X11Y101	42	mean 11/N 60	mean 3/N 5	mean 2/N 6	~60
	WS17-3-212-X57Y101	38	mean 7/N 37	mean 3/N 6	mean 2/N 7	37
	WS17-3-222-X40Y93	41	mean 9/N 33	mean 4/N 6	mean 3/N 7	33
	WS17-2-152-X62Y103-1	37	mean 8/N 35	mean 3/N 4	mean 2/N 3	35
	WS17-2-152-X62Y103-2	26	mean 6/N 27	mean 4/N 5	mean 2/N 6	27
	WS17-2-152-X62Y103-3	26	8/N 1	none	none	none
	WS17-2-152-X62Y103-4	35	3/N 1	none	mean 3/N 5	none
	WS17-2-152-X62Y103-5	37	mean 8/N 38	mean 5/N 9	mean 2/N 7	38
	WS17-2-152-X62Y103-6	42	mean 4/N 46	mean 2/N 6	mean 2/N 6	46
	WS17-2-160-X37Y98	35	mean 8/N 36	mean 3/N 7	mean 2/N 8	~36
	WS17-3-210-X52Y101	29	mean 9/N 23	mean 4/N 5	mean 3/N 5	~23
	WS17-3-212-X39Y94	none	5/N 1	none	none	none
	WS17-3-219-X56Y102	45	mean 5/N 49	mean 3/N 6	mean 3/N 9	49
	WS17-3-232-X24Y112	48	mean 7/N 60	mean 4/N 7	mean 3/N 7	60
	WS17-3-241-X45Y114	48	mean 12/N 43	mean 4/N 8	mean 2/N 5	43
	WS17-3-241-X45Y114-2	43	mean 6/N 60	mean 3/N 7	mean 2/N 7	> 60
	WS17-3-256-X30Y100	35	mean 8/N 32	mean 4/N 7	mean 3/N 7	32
	WS17-3-256-X30Y100-2	45	mean 10/N 30	mean 3/N 8	mean 2/N 6	> 80
	WS17-3-208-X53Y103	36	mean 8/N 31	mean 4/N 4	mean 3/N 7	31
	WS17-3-226-X27Y109	37	mean 8/N 36	mean 3/N 6	mean 2/N 6	36
	WS17-2-145-X41.5Y115	31	mean 6/N 12	mean 7/N 5	mean 4/N 8	12
	WS17-3-213-X59Y96	32	mean 7/N 27	mean 4/N 8	mean 3/N 7	27
Mengeosphaera membranifera Shang, Liu, and Moczydłowska, 2019	WS17-2-152-X62Y103	42	mean 4/N 46	mean 2/N 6	mean 2/N 6	46
	WS17-3-204-X37Y93	40	mean 7/N 48	mean 3/N 6	mean 2/N 6	48
	WS17-3-207X30Y104	40	mean 7/N 50	none	none	> 50
	WS17-3-231-X27Y101	48	mean 7/N 41	mean 4/N 7	mean 2/N 5	~41
Tanarium tuberosum Moczydłowska, Vidal, and Rudavskaya, 1993	WS17-3-201-X42.5Y93.5	91.64	mean 12/N 26	mean 6/N 6	mean 6/N 6	26
	WS17-3-202-X57Y93	111.9	mean 25/N 12	mean 23/N 5	mean 11/N 8	12
Tanarium conoideum Kolosova, 1991	WS17-2-150-X47Y101	43	mean 10/N 15	mean 8/N 9	mean 4/N 6	15
	WS17-2-150-X50Y111	37	9.14/N 1	none	6.04/N 1	none
	WS17-3-206-X25Y104	38	mean 8/N 21	mean 7/N 6	mean 3/N 6	21
	WS17-3-210-X38Y103	33	mean 9/N 7	mean 8/N 7	mean 3/N 7	7
	WS17-3-234-X46Y99	43	mean 10/N 19	mean 7/N 8	mean 4/N 8	19
	WS17-2-153-X56Y97	45	mean 9/N 27	mean 5/N 5	mean 2/N 4	27
Tanarium elegans Liu et al., 2014a	WS17-2-150-X59.5Y108	39	mean 7/N 35	mean 4.01/N 4	mean 2/N 4	35
	WS17-2-197-X61Y98	44	9.36/N 1	none	none	none
Estrella recta Liu and Moczyd-łowska, 2019	WS17-2-157-X64Y101	none	mean 26/N 11	mean 7/N 6	none	11
	WS17-2-195-X54Y99	36	mean 8/N 7	none	none	7
	WS17-3-225-X46Y106	45	mean 21/N 16	mean 11/N 7	mean 6/N 6	16
	WS17-3-259-X19.5Y113	49	mean 15/N 13	none	mean 4/N 8	~24
Variomargo-sphaeridium gracile Xiao et al., 2014a	WS17-2-150-X50Y110	43	mean 6/N 25	mean 3.574/N 5	mean 2/N 5	~25
	WS17-2-155-X27Y109	40	mean 11/N 31	mean 4.75/N 8	mean 3/N 7	31
	WS17-2-161-X48Y103	56	mean 10/N 52	mean 3.56/N 8	mean 3/N 6	52
	WS17-2-200-X28Y104	43	mean 11/N 36	mean 3.99/N 5	mean 2/N 7	36
	WS17-3-205-X57Y99	40	mean 10/N 33	mean 3.89/N 7	mean 2/N 8	33
	WS17-3-207-X17Y99	53	mean 12/N 48	mean 3.76/N 5	mean 3/N 6	48
	WS17-3-207-X28.5Y106	42	mean 10/N 36	mean 4.15/N 5	mean 3/N 6	36
	WS17-3-207X49Y103	37	mean 9/N 41	mean 4.21/N 6	mean 3/N 6	41
	WS17-3-223-X21Y103	none	mean 9/N 33	mean 4.00/N 8	mean 3/N 6	~33

https://doi.org/10.1017/jpa.2024.16 Published online by Cambridge University Press

Continued.

Taxon	Thin section no.	Vesicle diameter (μm)	Length of processes (mean μm/N)	Distance between processes (mean μm/N)	Basal width of process (mean μm/N)	Quantity of processes
	WS17-3-223-X22Y103	none	mean 12/N 40	mean 3.58/N 10	mean 3/N 7	40
	WS17-3-226-X52Y94	38	7/N 1	mean 4.96/N 6	mean 3/N 6	none
	WS17-3-234-X46Y99	41	mean 13/N 42	mean 3.41/N 7	mean 2/N 7	42
	WS17-3-256-X30Y100	34	mean 8/N 32	mean 3.97/N 7	mean 3/N 7	32
Weissiella cf. *W. grandistella* Vorob'eva, Sergeev, and Knoll, 2009	WS17-2-195-X54Y99	118	mean 33/N 4	mean 24.68/N 2	mean 13/N 5	8

Accepted: 9 February 2024

https://doi.org/10.1017/jpa.2024.16 Published online by Cambridge University Press